The following publication Wang, F. and Chan, T.L. (2023), "A new sorting algorithm-based merging weighted fraction Monte Carlo method for solving the population balance equation for particle coagulation dynamics", International Journal of Numerical Methods for Heat & Fluid Flow, Vol. 33 No. 2, pp. 881-911 is published by Emerald and is available at https://doi.org/10.1108/HFF-06-2022-0378.

A New Sorting Algorithm-based Merging Weighted Fraction Monte Carlo Method for Solving the Population Balance Equation for Particle Coagulation Dynamics

Fei Wang and Tat Leung Chan*

Department of Mechanical Engineering, The Hong Kong Polytechnic University

Hong Kong SAR, China

*Corresponding author: Tat L. Chan can be contacted at: mmtlchan@polyu.edu.hk

Abstract

Purpose: The purpose of this study is to present a newly proposed and developed sorting algorithm-based merging weighted fraction Monte Carlo (SAMWFMC) method for solving the population balance equation for the weighted fraction coagulation process in aerosol dynamics with high computational accuracy and efficiency.

Design/methodology/approach: In the new SAMWFMC method, the jump Markov process is constructed as the weighted fraction Monte Carlo (WFMC) (Jiang and Chan, 2021) method with a fraction function. Both adjustable and constant fraction functions are used to validate the computational accuracy and efficiency. A new merging scheme is also proposed to ensure a constant-number and constant-volume scheme.

Findings: The new SAMWFMC method is fully validated by comparing with existing analytical solutions for six benchmark test cases. The numerical results obtained from the SAMWFMC method with both adjustable and constant fraction functions show excellent agreement with the analytical solutions and low stochastic errors. Compared with the WFMC method (Jiang and Chan, 2021), the SAMWFMC method can significantly reduce the stochastic error in the total particle number concentration without increasing the stochastic errors in high-order moments of the particle size distribution (PSD) at only slightly higher computational cost.

Originality/value: The WFMC method (Jiang and Chan, 2021) has a stringent restriction on the fraction functions, making few fraction functions applicable to the WFMC method except for several specifically selected adjustable fraction functions, while the stochastic error in the total particle number concentration is considerable large. The newly developed SAMWFMC method shows significant improvement and advantage in dealing with weighted fraction coagulation process in aerosol dynamics and provides an excellent potential to deal with various fraction functions with higher computational accuracy and efficiency.

Keywords: Monte Carlo, Coagulation, Sorting algorithm, Merging scheme, Fraction functions

Paper type: Research paper

Nomenclature

C_0	total coagulation rate
C_{ij}	coagulation rate of numerical particles, i and j
i	numerical particle label
j	numerical particle label
M_k	kth order moment
n	particle size distribution function
N_0	initial total number concentration
P_k	probability of a particle containing k primary particles
Q	number of MC repetitions
r	random number
t	time
v_i	particle volume of the numerical particle, i
V	volume of the computational domain
w_i	weight of the numerical particle, i

Greek Letters

α	fraction function
β	coagulation kernel
σ	mean standard deviation

τ	waiting time
τ_c	characteristic coagulation time
Φ	coagulation rate
Ω	mean number of coagulation events

Glossary

CCK	constant coagulation kernel
CFF	constant fraction function
CPU	central processing unit
DSMC	direct simulation Monte Carlo
EFF	exponential fraction function
GDE	general dynamic equation
GPU	graphic processing unit
HFF	hyperbolic fraction function
HPC	high performance cluster
IED	initial exponential distribution
IMD	initial monodispersed distribution
LCK	linear coagulation kernel
MC	Monte Carlo
MFA	mass flow algorithm
MMC	multi-Monte Carlo
MOM	method of moment
OOP	object-oriented programming
PBE	population balance equation
PSD	particle size distribution
QCK	quadratic coagulation kernel
SAMWFMC	sorting algorithm-based merging weighted fraction Monte Carlo
SCFF	stepwise constant fraction function
SM	sectional method
WFA	weighted flow algorithm
WFMC	weighted fraction Monte Carlo

1. Introduction

Aerosol dynamics involve a great variety of areas in science and engineering including atmospheric aerosols, combustion-generated particles, aerosol reactors, chemical engineering,

nanoparticle synthesis and food processes (Friedlander, 2000). Aerosol dynamic processes including nucleation, condensation/evaporation (surface growth), breakage and coagulation generate and remove particles from the particle populations, which change the particle size distribution (PSD). The changes in the PSD function with time and position are governed by the population balance equation (PBE) (i.e., general dynamic equation (GDE)) (Friedlander, 2000). Coagulation is one of the most important aerosol dynamic-processes, which refers to two particles colliding to form a large one and leads to the decrease of the particle number and the increase of the average particle size. As a coagulation event always occurs between two particles, it is regarded as the most demanding event for modelling among various aerosol dynamic events (Xu *et al.*, 2014; Zhao *et al.*, 2009). The dynamic evolution of PSD due to coagulation is described by the so-called Smoluchowski coagulation equation as (Friedlander, 2000):

$$\frac{\partial n(v,t)}{\partial t}=\frac{1}{2}\int_0^v \beta(u,v\text{-}u,t)n(u,t)n(v\text{-}u,t)du - n(v,t)\int_0^\infty \beta(u,v,t)n(u,t)du \tag{1}$$

where $n(v,t)$ is the PSD function at time t; $n(v,t)dv$ is the particle number concentration with size range between v and $v+dv$ at time t; $\beta(u,v,t)$ is the collision frequency or coagulation kernel of two particles with volume u and v at time t which is a description of the coagulation rate.

The GDE is a nonlinear partial integro-differential equation of the PSD, whose analytical solution only exists in a few special cases (Friedlander, 2000; Liffman, 1992; Kruis *et al.*, 2000; Zhao *et al.*, 2005b; Ramabhadran *et al.*, 1976; Wang *et al.*, 2020) due to its complex characteristics. These existing analytical solutions are of great significance and can be used as a useful benchmark for validating different numerical methods. Different numerical approaches aiming at different problems of aerosol dynamics are developed to approximate the solution of the GDE for an aerosol system of interest, such as the sectional method (SM) (Gelbard *et al.*, 1980; Prakash *et al.*, 2003; Zhang *et al.*, 2020; Wu *et al.*, 2022), method of moments (MOMs) (Frenklach and Harris, 1987; McGraw, 1997; Yu *et al.*, 2008; Yu and Chan, 2015; Chan *et al.*, 2018; Li *et al.*, 2019; Liu *et al.*, 2019c; Shen *et al.*, 2020; Yang *et al.*, 2020; Jiang *et al.*, 2021; Shen *et al.*, 2022) and Monte Carlo (MC) method (Gillespie, 1975; Garcia *et al.*, 1987; Liffman, 1992; Smith and Matsoukas, 1998; Kruis *et al.*, 2000; Lin *et al.*, 2002; Zhao *et al.*, 2009; Xu *et al.*, 2014; Kotalczyk and Kruis, 2017; Liu and Chan, 2017; Liu and Chan, 2018a, 2018b; Liu *et*

al., 2019a, 2019b; Liu and Chan, 2020; Liu *et al.*, 2021; Jiang and Chan, 2021; Liu *et al.*, 2022). As the discrete nature of the MC method perfectly matches the stochastic properties of particle motion, it can be used to closely simulate the behaviour of particles.

Gillespie (1975) presented a MC algorithm for simulating the stochastic coagulation process in a cloud and described the computational procedures in detail, which formed the basis of the later development. However, the number of numerical particles used in the MC simulation is restricted to only 10^3-10^7 (Zhao and Zheng, 2009b) due to the limitation of the computer resources (i.e., central processing unit (CPU) speed and computer memory), the computational accuracy is unavoidably affected which is inversely proportional to the square root of the total number of numerical particles (Liffman, 1992).

Except for straightforwardly adopting high performance cluster (HPC) or graphic processing unit (GPU) (Kotalczyk and Kruis, 2017; Xu *et al.*, 2015; Kruis *et al.*, 2012) to speed up computations, improving or developing a better MC algorithm is still an effective measure to reduce the stochastic errors and to increase the computational accuracy as well as the computational efficiency. The coagulation event leads to a constant decrease in the particle numbers with a further reduction in the computational accuracy. In order to address this technical problem, Liffman (1992) developed a direct simulation Monte Carlo (DSMC) method, which uses a stepwise constant-number approach to avoid the continuous reduction of the particle numbers. Specifically, the number of numerical particles is doubled with all surviving particles copied and added to the computational domain for the conservation of statistical particle properties when the particle number in the computational domain is dropped by half. By comparison, Smith and Matsoukas (1998) introduced a continuous constant-number MC method, in which a numerical particle from the computational domain with the same probability is randomly selected and copied it to fill the position vacated by coagulation. Lin *et al.* (2002) proposed another constant-number MC method to maintain the particle number constant but continuously change the volume of the computational domain. Kruis *et al.* (2000) proposed and demonstrated a fast DSMC method for simulating complex particle systems, in which a doubling procedure is also included when the particle number is dropped by half. In fact, it is observed that the particle number concentration at

the edge of the PSD is normally very small in nature and its relevant engineering applications (Zhou *et al.*, 2020). Although these MC methods can achieve acceptable computational accuracy under this situation, some detailed information of real particles may be lost at the edge of the PSD because only several numerical particles are used to represent the real particles in this area, which leads to the deterioration of the statistical precision (Zhao and Zheng, 2009b). A multi-Monte Carlo (MMC) method was proposed for reducing the stochastic errors by introducing the concept of "weighted fictitious particles" (Zhao *et al.*, 2005a, 2005b; Zhao *et al.*, 2009). In the MMC method, the number of fictitious particles and the volume of the computational domain always keep constant, and each fictitious particle is a representative of some real particles. By providing different fictitious particles with different weights (Zhao and Zheng, 2009b; Xu *et al.*, 2014; Liu and Chan, 2017; Liu and Chan, 2018a, 2018b; Liu *et al.*, 2021), the weights of fictitious particles are unevenly distributed in the particle size spectrum (i.e., more fictitious particles at the edge of the PSD and fewer fictitious particles at those areas where the particle number concentration is high). Therefore, the statistically reasonable precision in less populated areas of the particle size spectrum can be guaranteed while the accuracy in densely populated areas is sufficient. Kotalczyk and Kruis (2017) presented a new numerical approach to calculate the coagulation rates of weighted particles by non-weighted particles, which an advantage in reducing statistical noise was shown. The mass flow algorithm (MFA) developed by Debry *et al.* (2003) can ensure convergence results due to its well found theoretical basis, which can be used as a reference solution for benchmarking other numerical methods. By comparison, DeVille *et al.* (2011) proposed the weighted flow algorithm (WFA) for the improvement in the computational efficiency, in which particle weighting functions with power laws in particle size were introduced. Zhou *et al.* (2020) reported that the weight function used in the MC method has a beneficial effect on the prediction of the PSD. Jiang and Chan (2021) have innovatively introduced fraction functions for particle weight functions, and applied it to a newly developed MC method called weighted fraction Monte Carlo (WFMC) (Jiang and Chan, 2021, 2022) method. Numerical results showed that the WFMC method can reduce the stochastic errors in high-order moments of the PSD by introducing adjustable fraction functions.

Although the introduction of adjustable fraction functions in the WFMC method are conducive to the computational accuracy of high-order moments of the PSD, the stochastic error in the total particle number concentration significantly increases which is always much larger than the DSMC and MMC methods (Jiang and Chan, 2021). In addition, the WFMC method has a rigid limitation on the fraction functions, making few fraction functions applicable to the WFMC method except for those specifically selected adjustable fraction functions. For example, if the fraction function is a constant which is not equal to 1, a large statistical noise or even error will be shown. This significantly reduces the generality of fraction functions and limits the applicability of the WFMC method. To tackle these problems, a new sorting algorithm-based merging weighted fraction Monte Carlo (SAMWFMC) method is proposed and developed in the present study. Three adjustable fraction functions applicable to the WFMC method and constant fraction functions are also introduced to check the reliability of the SAMWFMC method. A new merging scheme is then proposed and developed to ensure a constant-number and constant-volume scheme. Six benchmark test cases with existing analytical solutions are used to validate the newly developed SAMWFMC method and the resulting stochastic errors are also compared with those of the DSMC, MMC and WFMC methods.

2. Development of the New Sorting Algorithm-based Merging Weighted Fraction Monte Carlo (SAMWFMC) Method

In MC methods for particle coagulation, the construction of a jump Markov process depends on the coagulation rate between numerical particles with different particle weights, because the coagulation rate determines the time step between two successive coagulation events and the selection of a coagulation particle pair. The development of the new SAMWFMC method is presented.

2.1. Calculation of the coagulation rate

A numerical particle, i is a representative of a group of real particles with the number equals to w_i and the volume equals to v_i. The real particle number concentration of this group is w_i/V, where V is the volume of the computational domain. Similarly, w_j/V is the real particle number concentration of a group represented by the numerical particle, j. Therefore, the number of coagulation events among real particles per unit time and volume between ith-group and jth-group of numerical particles can be

expressed by (Zhao *et al.*, 2009):

$$\Phi_{ij}=\beta_{ij}\times\frac{w_i}{V}\times\frac{w_j}{V} \tag{2}$$

where Φ_{ij} is the coagulation rate between a random chosen real particle from the ith-group and a random chosen real particle from the jth-group, while β_{ij} is the coagulation kernel function of particles i and j. Thus, the number of coagulation events of the real particles between the ith-group and jth-group per unit time in the computational domain is $V\Phi_{ij}$.

In the present study, it is considered that coagulation events occur among a part of or all real particles between the ith-group and jth-group, which is characterized by a fraction function, α_{ij} (Jiang and Chan, 2021, 2022). The mean number of coagulation events within these real particles is given by (Jiang and Chan, 2021):

$$\Omega=\alpha_{ij}\min\left(w_i,w_j\right),\alpha_{ij}\in(0,1] \tag{3}$$

Therefore, the number of coagulation events of the real particles between the ith-group and jth-group per unit time in the computational domain can also be formulated by ΩC_{ij} (Jiang and Chan, 2021):

$$V\Phi_{ij}=\Omega C_{ij} \tag{4}$$

where C_{ij} is the coagulation rate between numerical particles, i and j, which can be written as (Jiang and Chan, 2021):

$$\begin{aligned} C_{ij}&=\frac{\max\left(w_i,w_j\right)}{\alpha_{ij}}\frac{\beta_{ij}}{V}=\frac{\beta'_{ij}}{V}\\ \beta'_{ij}&=\frac{\max\left(w_i,w_j\right)}{\alpha_{ij}}\beta_{ij} \end{aligned} \tag{5}$$

where β_{ij}' is the new coagulation kernel function which is used to construct the jump Markov process.

2.2. Determination of a time step

The waiting time between two events (i.e., coagulation) is an exponentially distributed random variable as (Gillespie, 1975):

$$P(\tau) = C_0 \exp(-C_0\tau) \tag{6}$$

where C_0 is the total coagulation rate which is written as (Gillespie, 1975):

$$C_0 = \sum_{i=1}^{N-1} \sum_{j=i+1}^{N} C_{ij} \tag{7}$$

Therefore, the occurrence probability of a coagulation event of numerical particles, $P_{\text{coag}}(\Delta t)$ in the computational domain with a volume of V and within a time step of Δt is given by (Jiang and Chan, 2021):

$$P_{\text{coag}}(\Delta t) = 1 - \exp(-\Delta t C_0) \tag{8}$$

The time step is then determined as (Gillespie, 1975; Garcia *et al.*, 1987):

$$\Delta t = \frac{\ln(1/r_1)}{C_0} \tag{9}$$

where r_1 is a random number from the uniform distribution between zero and one.

2.3. Selection of a coagulation particle pair

The acceptance-rejection method (Garcia *et al.*, 1987) and the cumulative probability method (i.e., the inverse method) (Liffman, 1992) are two commonly used for selecting a coagulation pair at random basis. Since the inverse method needs to calculate the coagulation rates of all possible particle pairs which is time-consuming (Kruis *et al.*, 2000), the acceptance-rejection method is then adopted in the present study. At first, the numerical particles, i and j, are randomly selected, and then they would be accepted as a numerical particle pair to conduct a coagulation event if the following condition is satisfied as (Garcia *et al.*, 1987; Gillespie, 1975):

$$r_2 \le \frac{C_{ij}}{\max\limits_{\forall k, \forall m} C_{km}} \tag{10}$$

where r_2 is a random number from the uniform distribution in the unit interval. Otherwise, they are rejected, and then a new numerical particle pair is entirely selected at random basis to repeat the acceptance or rejection procedure until a satisfied numerical particle pair is obtained. It should be noted

that the Markov process still can be exactly implemented even though the $\max_{\forall k,\forall m} C_{km}$ in Equation (10) is overestimated (Garcia *et al.*, 1987; Xu *et al.*, 2014).

2.4. Fraction functions

In the WFMC method, three types of adjustable fraction functions (i.e., hyperbolic fraction function (HFF), exponential fraction function (EFF) and stepwise constant fraction function (SCFF)) with a rigid assumption are specially selected (Jiang and Chan, 2021) as presented in Equations (11) to (13). It should be noted that all these three types of adjustable fraction functions have a specific range from 0.5 to 1 closely related to the volumes of numerical particles i and j, which may lead to a totally different value of each numerical particle from others. In addition, all these fraction functions for numerical particles with large size discrepancy are strictly restricted to almost 1, which means that a numerical particle pair with small size difference undergoes a weighted fraction coagulation event while two numerical particles of large size discrepancy do not experience a weighted fraction coagulation. From this point of view, all these fraction functions are used to control the coagulation process of a numerical particle pair in terms of its volume ratio in the WFMC method. This is the prerequisite of adopting the WFMC method (Jiang and Chan, 2021). If this rule is not followed, the WFMC method can lead to a very large statistical noise or even error and cannot be used for simulating coagulation anymore. This is the reason why only a few fraction functions (i.e., HFF, EFF and SCFF) are applicable to the WFMC method. Actually, even though these three types of adjustable fraction functions are used in the WFMC method, the stochastic error in the total particle number concentration is still large (Jiang and Chan, 2021).

In the present study, these three types of adjustable fraction functions (HFF, EFF and SCFF) are used in the newly proposed and developed SAMWFMC method to validate the computational accuracy and efficiency. Meanwhile, constant fraction functions (CFF) in Equation (14) are also introduced to extend the generality of the fraction functions and check the applicability of the new SAMWFMC method. It should be noted that C in Equation (14) can be an arbitrary number between zero and unity, which is consistent with the expression in Equation (3).

$$\alpha_{ij}=\frac{1}{1+\min(v_i,v_j)/\max(v_i,v_j)} \tag{11}$$

$$\alpha_{ij}=1-2^{-\max(v_i,v_j)/\min(v_i,v_j)} \tag{12}$$

$$\alpha_{ij}=\begin{cases}0.5, & \max(v_i,v_j)/\min(v_i,v_j)\le 2\\ 1, & \max(v_i,v_j)/\min(v_i,v_j)>2\end{cases} \tag{13}$$

$$\alpha_{ij}=C \tag{14}$$

2.5. A new merging scheme

Every time when a numerical particle pair undergoes a weighted fraction coagulation event, there is an additional new numerical particle generated in the computational domain, leading to the continuous increasing in the number of numerical particles when more coagulation events occur. As a result, the computational efficiency will drop. It should be noted that the additional numerical particle with the lowest weight after a coagulation event is represented by "New *x*" as shown in Figure 1. In order to keep the number of numerical particles constant in the constant computational domain, Jiang and Chan (2021) have recently proposed a probabilistic removal scheme by randomly removing one of the coagulated numerical particles ("New *i*" or "New *j*" as shown in Figure 1) out of the computational domain and then adjusting the weight of the other coagulated numerical particle after the coagulation event. However, this probabilistic removal scheme may result in the fluctuation of the total particle number concentration.

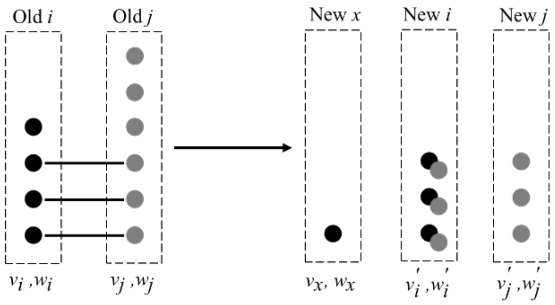

Figure 1 Schematic diagram of numerical particles undergoing a weighted fraction coagulation.

In the present study, a new merging scheme is proposed and developed to ensure a constant-number and constant-volume scheme. If the fraction function is equal to 1 and the weights of two

coagulated numerical particles are equal, it is straightforward to distribute the equal volume and weight to the two new numerical particles as shown in Figure 2. Otherwise, the schematic diagrams of the merging scheme in terms of different volumes and weights of a coagulated numerical particle pair are shown in Figures 3 and 4. Instead of removing one coagulated numerical particle out of the computational domain in the WFMC method (Jiang and Chan, 2021), the idea of the merging scheme in the present study is to add the "New x" in Figure 1 to an existing numerical particle in the computational domain.

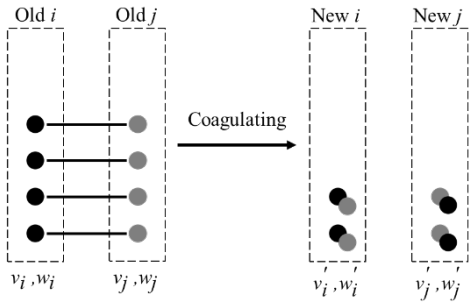

Figure 2 Schematic diagram of merging weighted fraction when $\alpha_{ij} = 1$ and $w_i = w_j$.

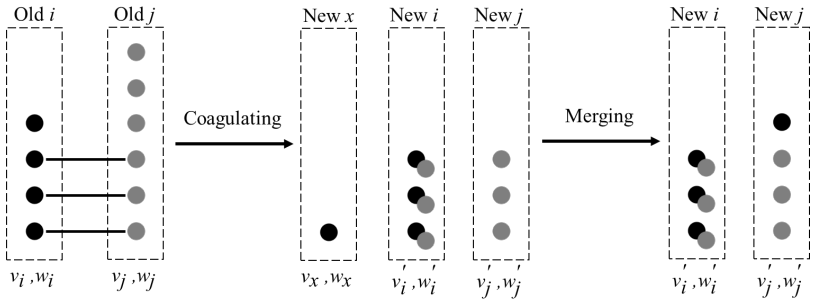

(a) $w_i \leq w_j$

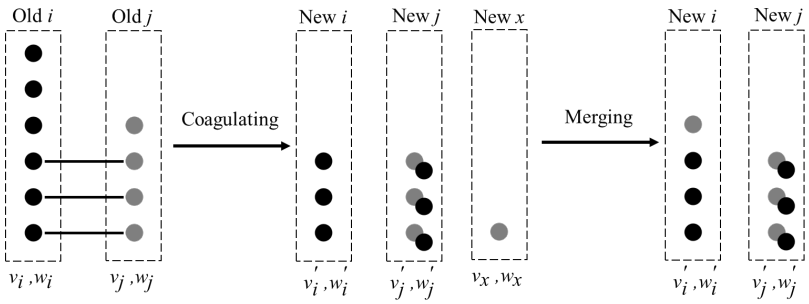

(b) $w_i > w_j$

Figure 3 Schematic diagram of merging weighted fraction when $v_i = v_j$.

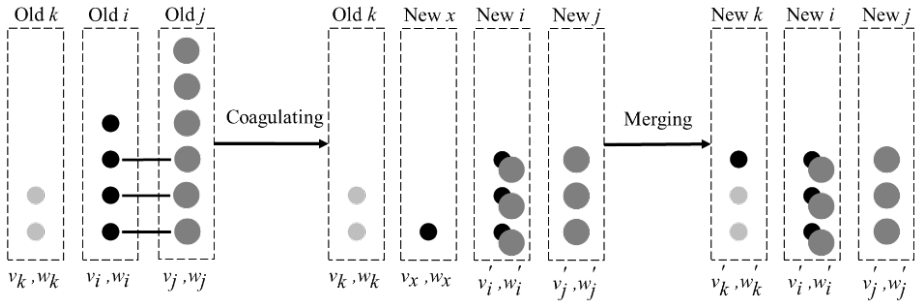

(a) $w_i \leq w_j$

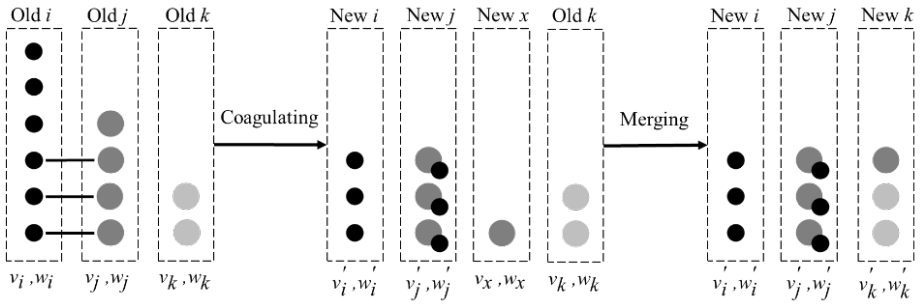

(b) $w_i > w_j$

Figure 4 Schematic diagram of merging weighted fraction when $v_i \neq v_j$.

If the volumes of two coagulated numerical particles are equal, only these two coagulated numerical particles are required to be involved in the merging scheme. If the weight of the "Old *i*" is not larger than that of the "Old *j*" as shown in Figure 3(a), the "Old *i*" will be replaced by the "New *i*" with the volume equal to $(v_i + v_j)$, and the "New *x*" will be added to the "Old *j*" and the "New *j*" will then be formed. If the weight of the "Old *i*" is larger than that of the "Old *j*" as shown in Figure 3(b), the "Old *j*" will be replaced by the "New *j*" with the volume equals to $(v_i + v_j)$, and the "New *x*" will be added to the "Old *i*" and the "New *i*" will then be formed.

By comparison, the handling of the "New *x*" is completely different when the volumes of these two numerical particles, v_i and v_j, are not equal. Under this circumstance, a totally new numerical particle, "Old *k*", neither "Old *i*" nor "Old *j*", in the computational domain is introduced to implement the merging scheme as shown in Figure 4. If the weight of the "Old *i*" is not larger than that of the "Old *j*" as shown in Figure 4(a), the "Old *i*" will be replaced by the "New *i*" with the volume equal to $(v_i + v_j)$, the "Old *j*" will be replaced by the "New *j*" with the same volume v_j, and the "New *x*" will be added to the "Old *k*" and the "New *k*" will then be formed. But if the weight of the "Old *i*" is larger than

that of the "Old *j*" as shown in Figure 4(b), the "Old *j*" will be replaced by the "New *j*" with the volume equals to ($v_i + v_j$), and the "Old *i*" will be replaced by the "New *i*" with the same volume v_i and the "New *x*" will be added to the "Old *k*" and the "New *k*" will then be formed.

Therefore, the choice of the numerical particle, "Old *k*" becomes of great importance in the merging scheme because a randomly chosen "Old *k*" in the computational domain undoubtedly leads to the introduction of large statistical noise. However, if the volume of the "Old *k*" is close or equal to that of the "New *x*", the statistical noise of the new merging scheme can significantly reduce. Clearly, the most appropriate "Old *k*" has the same properties as the "New *x*" or has the nearest properties to the "New *x*", so the property (i.e., volume) difference between the "New *x*" and "Old *k*" is defined as:

$$S_x = |v_k - v_x| \tag{15}$$

when S_x is the minimal where the corresponding *k* is the most appropriate numerical particle for "New *x*" to be merged.

It should be noted that the volume of the "New *k*" is treated as the same as the "Old *k*" after merging, while the weight of the "New *k*" would be adjusted according to the volume/mass conservation rule, which will be presented later in Section 2.7. Therefore, the newly proposed merging scheme in the present study is completely different from those used in Kotalczyk and Kruis (2017) and Zhao *et al.* (2005a). In order to deal with an additional numerical particle generated by a breakage event, Zhao *et al.* (2005a) adopted a merging measure where the number of numerical particles is kept to be constant by directly adding the weights of the additional numerical particle and a randomly selected one with the similar volume together. Although the total particle number concentration is conserved exactly, the stochastic error in the total particle volume/mass concentration may occur. By comparison, Kotalczyk and Kruis (2017) introduced a technique of merging a generated numerical particle due to nucleation, breakage or transport to conserve both the total particle number and volume/mass densities, but the purpose of each merging treatment is to reduce one numerical particle and vacate a position in the computational domain by selecting two existing numerical particles to form a new one. But these two existing numerical particles should be specially selected; otherwise a very large stochastic noise or even error would be introduced. A low weight merging scheme is then introduced to minimise the stochastic

error, in which the most appropriate merging numerical particle pair should be determined by comparing all possible numerical particle pairs. If the number of numerical particles used is N, the number of comparisons in numerical particle pairs is then $N(N\text{-}1)$, which is very computationally expensive. Although the time complexity of this merging scheme is reduced to $O(\log N)$ which can be achieved to accelerate computations by using both parallel computing and graphic processing units (GPUs), the whole algorithm and programming are fairly complex.

Obviously, it is not sensible to compare the properties of all the numerical particles one-by-one with that of "New x" because it is highly time-consuming, especially when the number of numerical particles is large. But if the properties (i.e., volume and weight) of numerical particles are sorted and stored in the computer memory, it is more convenient to find the target "Old k" by adopting the 1-nearest neighbour (1-NN) algorithm. In Figure 4(a), if the "Old k" is one of the nearest neighbours of the "Old i", it is obvious that the "Old k" has a similar volume with the "New x". Therefore, the "Old k" can be determined by:

$$k = \begin{cases} i\text{-}1, & S_{i\text{-}1} < S_{i+1} \\ i+1, & S_{i\text{-}1} \geq S_{i+1} \end{cases} \tag{16}$$

Similarly, the "Old k" in Figure 4(b) is determined as:

$$k = \begin{cases} j\text{-}1, & S_{j\text{-}1} < S_{j+1} \\ j+1, & S_{j\text{-}1} \geq S_{j+1} \end{cases} \tag{17}$$

Therefore, the sorting algorithm-based merging weighted fraction scheme is newly proposed and developed for easily and rapidly determining the target "Old k" with the nearest property to the "New x" by using 1-NN algorithm.

2.6. Selection of a sorting algorithm

As sorting numerical particles is vital to the computational accuracy in the newly developed SAMWFMC method, the selection of the most efficient sorting algorithm is essentially required for reducing the computational cost.

As discussed in the Section 2.5, the number of numerical particles remains constant during the numerical simulation by introducing the new merging scheme, so there is no need to implement the operation of adding or removing numerical particles anymore. This feature matches well with the data structure of array in the computer programming. More importantly, array supports random access, which implies that every numerical particle can be directly accessed by its index, which can significantly improve computational efficiency especially when the number of numerical particles is large. An object-oriented programming (OOP) language, C++ has classes and objects. A class is a type of data which includes properties and functions while an object is an instance of a class. In the present study, a class of the numerical particle including properties (e.g., identification number (ID), volume and weight) is defined. Then each object is created as an instance of the numerical particle class. Finally, an array is used to store a collection of objects of the numerical particle class.

As the prerequisite of implementing the merging scheme is that the numerical particle array should be sorted, it is necessary to sort the numerical particle array before the next coagulation event. Note that it is unnecessary to sort the initial numerical particle array if the initial PSD is monodispersed; otherwise, sorting the initial numerical particle array is required when the initial numerical particle system is generated. In the present study, the numerical particles are sorted by their properties (i.e., volume and weight), so all numerical particles are in order in terms of their properties. When two numerical particles, "Old i" and "Old j" with the same volume coagulate as shown in Figures 2 and 3, they are replaced in place by the "New i" and "New j"; otherwise, the "Old i", "Old j" and "Old k" are replaced in place by the "New i", "New j" and "New k" after coagulation as shown in Figure 4. Other numerical particles in the array remain constant, which demonstrate that there are only two or three numerical particles required to be sorted, so only an efficient sorting algorithm for the nearly sorted numerical particle array is needed.

There are a great variety of sorting algorithms such as bubble sort, selection sort, insertion sort, merge sort, heapsort and quicksort, and their variations (Sedgewick and Wayne, 2011) as there is no one sorting method that can deal with every situation (Goel and Kumar, 2018). The performance of a sorting algorithm is evaluated by the complexities of time and space in the notation of the standard big

O(n), where n is the size of the input data (Kapur *et al.*, 2012). The average time complexities of the bubble, selection and insertion sorts are O(n^2) while the average time complexities of the merge sort, heapsort and quicksort are O($n$log$n$). But, if the array is nearly or completely sorted, the time complexities of the selection sort, merge sort, heapsort and quicksort remain unchanged, while the time complexities of the bubble and insertion sorts become O(n), which implies that bubble and insertion sorts have high efficiency for nearly or completely sorted arrays (Cook and Kim, 1980). It is worth noting that both bubble and insertion sorts aim at small numbers of elements in the array. It is better to choose a suitable sorting algorithm with the time complexity of O($n$log$n$) when the number of elements needed to be sorted is large. In addition, the bubble sort adopts the exchanging method when sorting, which is not as efficient as the insertion method by the insertion sort. Therefore, in the newly proposed and developed SAMWFMC method, the insertion sort is used to sort the numerical particle array after a coagulation event is taken place as the numerical particle array is already in order except for only two or three numerical particles. Furthermore, if the initial PSD is not monodispersed, the quicksort is adopted to sort the initial numerical particle array after the numerical particle system is generated.

2.7. Treating a coagulation event

If two numerical particles undergo a coagulation event, the real particles represented by these two numerical particles also experience coagulation, which leads to the change in the properties (i.e., volume and weight) of these two numerical particles. If the fraction function, α_{ij} in Equation (3) is equal to 1 and the weights of "Old i" and "Old j" are the same as shown in Figure 2, all real particles would be coagulated. The consequence of this coagulation event is denoted as (Zhao *et al.*, 2009):

$$\text{if } w_i = w_j, \begin{cases} v_i' = v_i + v_j, \; w_i' = w_i/2 \\ v_j' = v_i + v_j, \; w_j' = w_j/2 \end{cases} \tag{18}$$

Otherwise, two or three numerical particles are involved as shown in Figures 3 and 4. The volume/mass of the "New x" is $(w_i\text{-}\alpha_{ij}w_i)v_i$ in Figures 3(a) and 4(a), and $(w_j\text{-}\alpha_{ij}w_j)v_j$ in Figures 3(b) and 4(b), respectively, which is merged with a selected numerical particle based on mass conservation, so the consequence of a coagulation event in terms of merging scheme is formulated as:

$$\text{if } v_i = v_j \text{ and } w_i \le w_j, \begin{cases} v_i' = v_i + v_j,\ w_i' = \alpha_{ij} w_i \\ v_j' = v_j, w_j' = w_j - \alpha_{ij} w_i + (w_i - \alpha_{ij} w_i)\dfrac{v_i}{v_j} = w_i + w_j - 2\alpha_{ij} w_i \end{cases} \tag{19}$$

$$\text{if } v_i = v_j \text{ and } w_i > w_j, \begin{cases} v_i' = v_i, w_i' = w_i - \alpha_{ij} w_j + (w_j - \alpha_{ij} w_j)\dfrac{v_j}{v_i} = w_i + w_j - 2\alpha_{ij} w_j \\ v_j' = v_i + v_j,\ w_j' = \alpha_{ij} w_j \end{cases} \tag{20}$$

$$\text{if } v_i \ne v_j \text{ and } w_i \le w_j, \begin{cases} v_i' = v_i + v_j,\ w_i' = \alpha_{ij} w_i \\ v_j' = v_j, w_j' = w_j - \alpha_{ij} w_i \\ v_k' = v_k, w_k' = w_k + (w_i - \alpha_{ij} w_i)\dfrac{v_i}{v_k} \end{cases} \tag{21}$$

$$\text{if } v_i \ne v_j \text{ and } w_i > w_j, \begin{cases} v_i' = v_i, w_i' = w_i - \alpha_{ij} w_j \\ v_j' = v_i + v_j,\ w_j' = \alpha_{ij} w_j \\ v_k' = v_k, w_k' = w_k + (w_j - \alpha_{ij} w_j)\dfrac{v_j}{v_k} \end{cases} \tag{22}$$

It should be noted that if the fraction function, α_{ij} is always equal to 1, the Equations (18) to (22) are completely consistent with those of the MMC method (Zhao *et al.*, 2009), which demonstrate that the MMC method is only a special case of the newly proposed SAMWFMC method when $\alpha_{ij} = 1$.

Every time when a coagulation event takes place, the coagulation rate C_{ij} in Equation (5), the total coagulation rate, C_0 in Equation (7) and $\max\limits_{\forall k, \forall m} C_{km}$ in Equation (10) should be recalculated since there are two or three numerical particles in the array whose volumes and weights are changed in the SAMWFMC method. In the present study, the smart bookkeeping technique (Kruis *et al.*, 2000) is used to calculate C_0 in Equation (7) and $\max\limits_{\forall k, \forall m} C_{km}$ in Equation (10), which can avoid spending a large amount of time for recalculating the coagulation rates, C_{ij} of those uncoagulated numerical particles. More specifically, double traversing and counting on each numerical particle from the beginning to the end only takes place in the initial calculation of the total coagulation rate, C_0 and there is no further double traversing and counting anymore during the numerical simulation.

2.8. Description of the SAMWFMC algorithm

Figure 5 shows the flowchart of the newly proposed and developed SAMWFFC algorithm for particle coagulation. More specifically, the full algorithm is described as follows.

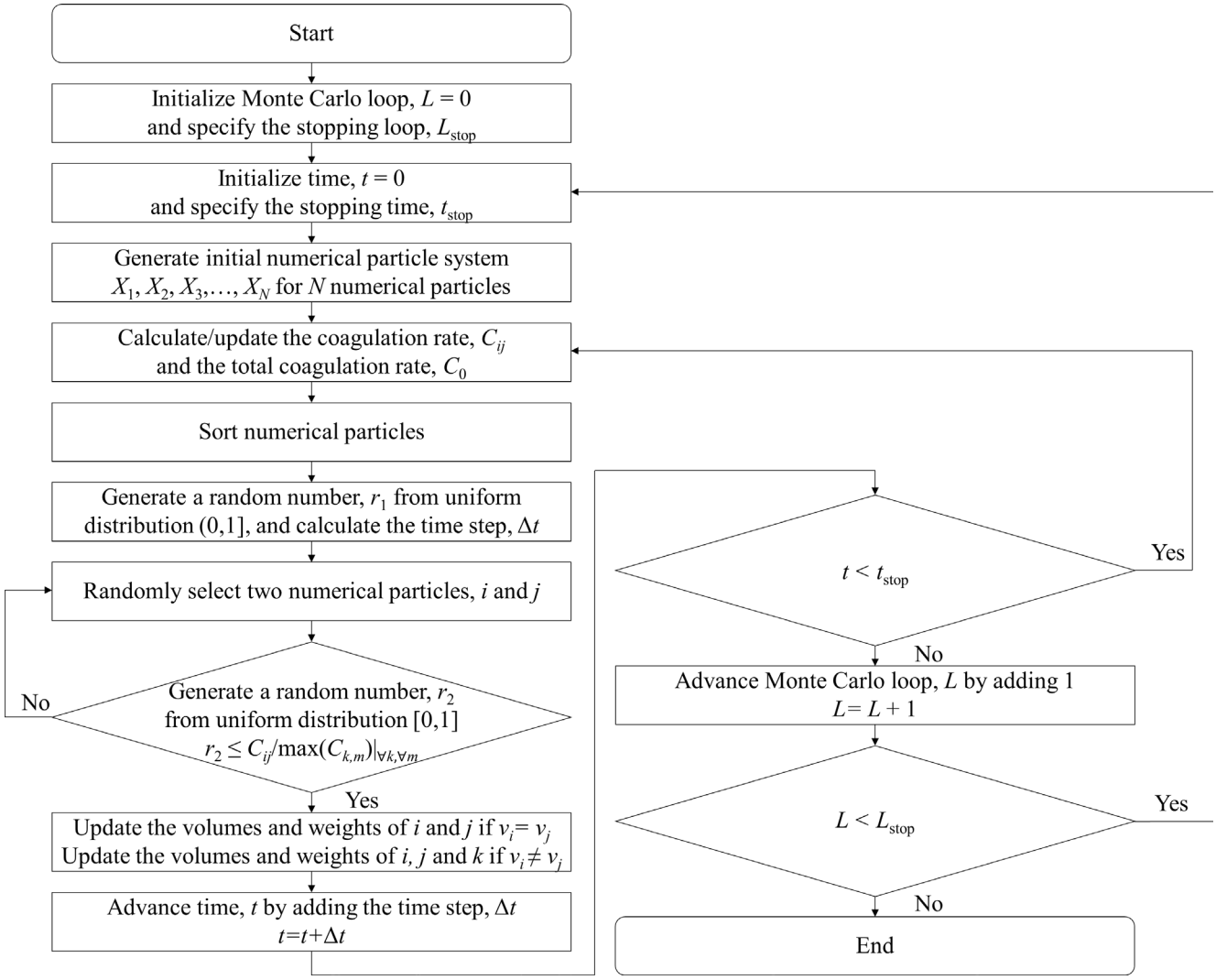

Figure 5 Flowchart of the newly proposed and developed SAMWFMC algorithm.

3. Results and Discussion

In the present study, two initial particle size distributions (i.e., initial monodispersed distribution (IMD) and initial exponential distribution (IED)), three coagulation kernels (i.e., constant coagulation kernel (CCK), linear coagulation kernel (LCK) and quadratic coagulation kernel (QCK)) and four fraction functions (i.e., hyperbolic fraction function (HFF), exponential fraction function (EFF), stepwise constant fraction function (SCFF) and constant fraction function (CFF)) are completely used. The newly proposed SAMWFMC method is fully validated by comparing the numerical results of the PSD and corresponding different orders of moments with the existing analytical solutions (Liffman, 1992; Zhao *et al.*, 2005b) to assess the computational accuracy. In addition, a comparison of stochastic

errors as well as computational efficiency with the DSMC (Kruis *et al.*, 2000), MMC (Zhao *et al.*, 2009) and WFMC (Jiang and Chan, 2021) methods is performed. The general moment of the PSD function can be expressed as (Friedlander, 2000):

$$M_k = \int_0^\infty v^k n(v)\,\mathrm{d}v \tag{23}$$

where k is the order of the moment. Different order moments normally have their specific physical meanings. For example, the zeroth moment, M_0 and the first moment, M_1 are the total particle number and mass (volume) densities, respectively. The mean standard deviations of the M_k are denoted as σ_{M_k} (Xu *et al.*, 2014; Zhao *et al.*, 2009; Zhao and Zheng, 2009a).

$$\sigma_{M_k}(t) = \frac{1}{Q}\sum_{i=1}^{Q}\sqrt{\frac{1}{t}\int_0^t\left[\frac{M_k^{\mathrm{MC}(i)}(t) - M_k^{\mathrm{AS}}(t)}{M_k^{\mathrm{AS}}(t)}\right]^2 \mathrm{d}t} \tag{24}$$

where Q is the number of MC repetitions. The analytical solution is represented by "AS" while MC(i) is the numerical results of the i-th MC simulation. In the present study, the number of MC repetitions used for all studied cases is 200 for achieving good enough stable mean standard deviations. The initial number of numerical particles used in the present study is 2000 (Kruis *et al.*, 2000; Zhao and Zheng, 2009a, 2009b; Zhao *et al.*, 2009; Kotalczyk and Kruis, 2017; Liu and Chan, 2017; Liu and Chan, 2018a; Zhou *et al.*, 2020) for all MC methods, which can achieve highly accurate numerical results.

3.1. Case 1: Initial monodispersed distribution and constant coagulation kernel function

Aerosols composed of particles with all the same size are called monodisperse aerosols. A typical case with the initial monodispersed distribution (IMD) and constant coagulation kernel (CCK) function is a benchmark for algorithm validation, as the analytical solution of the Smoluchowski equation exists (Liffman, 1992). In this case, the initial total particle number concentration, $N_0 = 10^6$ particles/cm^3 (Kruis *et al.*, 2000) and the coagulation kernel β_{ij} is equal to a constant A where $A = 10^{-6}$ cm^3/s (Kruis *et al.*, 2000). The characteristic coagulation time is defined as $\tau_c = 1/(AN_0)$.

Figure 6 shows the time evolutions of zeroth-order to third-order moments (i.e., M_0, M_1, M_2 and M_3) obtained from DSMC, MMC, WFMC and SAMWFMC methods and their corresponding mean

standard deviations (i.e., σ_{M_0}, σ_{M_1}, σ_{M_2} and σ_{M_3}) for different fraction functions (i.e., HFF, EFF, SCFF and CFF) with the IMD and CCK when compared with analytical solutions (Liffman, 1992). In Figure 6(a), the total particle number concentrations, M_0 for all studied MC methods decrease over time and show excellent agreement with the analytical solution due to the reduction in the number of real particles in each coagulation process. But the mean standard deviations, σ_{M_0} vary for different MC methods. It can be found that the σ_{M_0} obtained from the new SAMWFMC method are always lower than the counterparts of WFMC method (Jiang and Chan, 2021), which demonstrates that the SAMWFMC method always has higher computational accuracy in predicting M_0 than the WFMC method. Especially, the σ_{M_0} for the WFMC method with the HFF is the largest, even larger than that of the DSMC method, and keeps increasing with time, which are also found in Jiang and Chan (2021). It implies that the stochastic error in M_0 for the WFMC method with the HFF is very large and this method cannot allow for indefinitely long numerical simulations of the particle coagulation. It is because more coagulation events will occur with time advancing, the stochastic error will be even larger and the computational accuracy will be further reduced. By comparison, the σ_{M_0} for the SAMWFMC method with the HFF still remains at a very low stochastic error level and nearly unchanged with time, which demonstrates that the new merging scheme implemented in the proposed SAMWFMC method can effectively reduce the stochastic error in M_0. More importantly, as the WFMC method is not applicable to a CFF due to the limitation of the particle size discrepancy while the applicability of the SAMWFMC method is fully assessed for different CFFs (i.e., C = 0.5, 0.6, 0.7, 0.8 and 0.9) in the present study. It is found that different constants of the CFF have little effect on the σ_{M_0}, as all the σ_{M_0} obtained from the SAMWFMC method with C = 0.5 to 0.9 are very close and lower than that of the MMC method (Zhao *et al.*, 2009). As the coagulation process does not change the total volume/mass of numerical particles due to volume/mass conservation, the total volume concentrations, M_1 for all MC methods remain constant during the numerical simulation, therefore leading to no stochastic error in M_1 as shown in Figure 6(b).

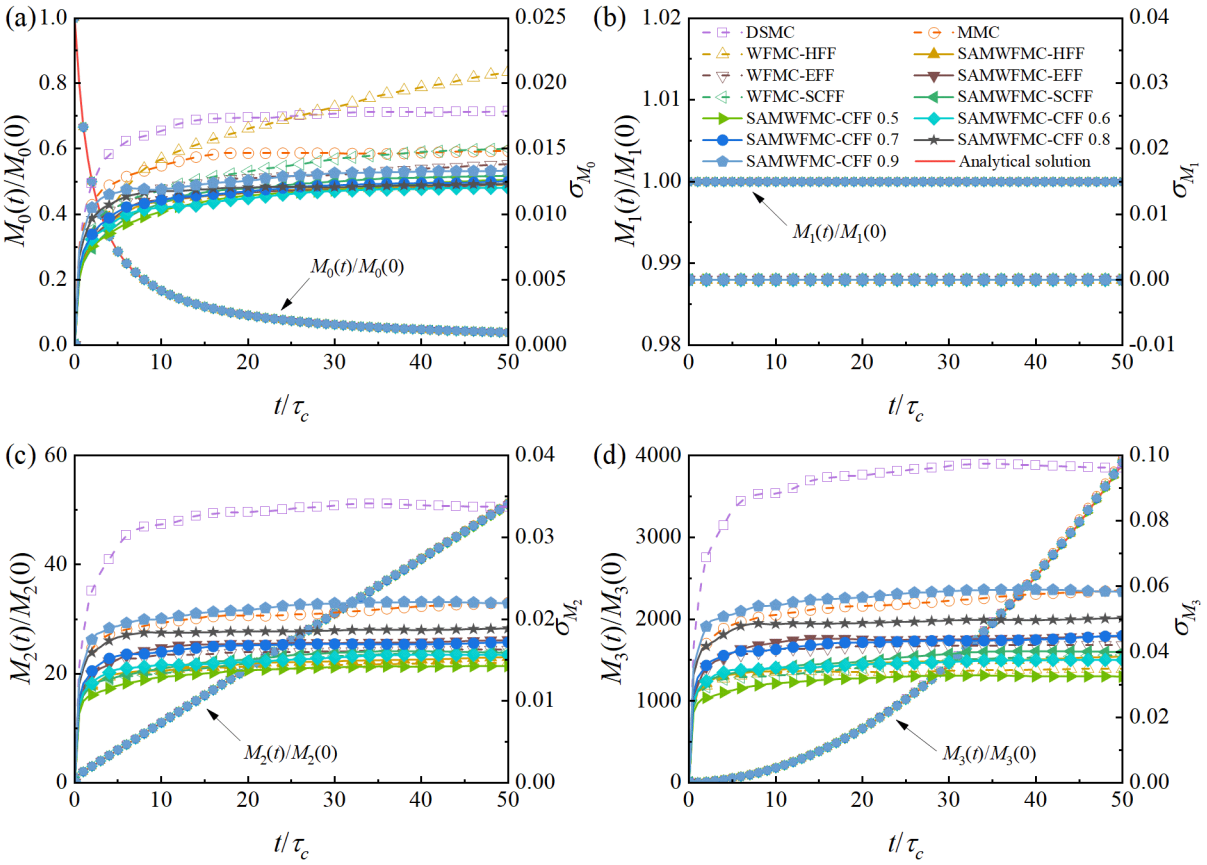

Figure 6 Time evolutions of zeroth-order to third-order moments and mean standard deviations obtained from DSMC, MMC, WFMC and SAMWFMC methods for different fraction functions with the IMD and CCK when compared with analytical solutions.

In Figures 6(c) and (d), the time evolutions of higher-order moments (i.e., M_2 and M_3) obtained from different MC methods are also in very good agreement with the analytical solutions. The DSMC method has the largest σ_{M_2} and σ_{M_3} than other MC methods, while the σ_{M_2} and σ_{M_3} obtained from the both WFMC and SAMWFMC methods are lower than those of the MMC method, which demonstrates that the introduction of the fraction function in the both WFMC and SAMWFMC methods has a significant reduction of stochastic errors in the higher-order moments. When the fraction function (i.e., HFF, EFF or SCFF) used in both WFMC and SAMWFMC methods is the same, the σ_{M_2} and σ_{M_3} for the SAMWFMC method are only slightly larger than those of the WMFC method, respectively, which implies that the new SAMWFMC method can achieve almost the same computational accuracy as the WFMC method. Furthermore, the effect of different CFFs for the SAMWFMC method on the σ_{M_2} and σ_{M_3} is also studied. Results show that with the CFF, the σ_{M_2} and σ_{M_3} obtained from the SAMWFMC

method with $C = 0.5$ are the lowest, and the σ_{M_2} and σ_{M_3} gradually increase with increasing C from 0.5 to 0.9. When $C = 0.9$, the σ_{M_2} and σ_{M_3} for the SAMWFMC method are almost equal to those of the MMC method.

Figure 7 shows the probabilities of obtaining a cluster containing k primary particles, P_k obtained from DSMC, MMC, WFMC and SAMWFMC methods for different fraction functions (i.e., HFF, EFF, SCFF and CFF) at $t/\tau_c = 50$ when compared with the analytical solution (Liffman, 1992), where P_k represents the PSD at $k = v/v_0$. Results show that all MC methods follow the analytical solution and track the PSD well, but there are varying degrees of fluctuations in the PSD for different MC methods. The DSMC method is found to have the narrowest PSD and the MMC method is slightly wider, the fluctuation in the PSD for the latter is smaller than the former when the particle size is the same at the high-end of the PSD. It can be also found that larger size particles can be obtained in both WFMC and SAMWFMC methods than those in the DSMC and MMC methods, so both WFMC and SAMWFMC methods with different fraction functions have wider PSDs than the MMC method, which implies that the introduction of the fraction function can significantly extend the prediction range of the PSD. When the fraction function used in the WFMC and SAMWFMC methods is the same (i.e., HFF, EFF or SCFF), the SAMWFMC method has almost the same wide PSDs as the WFMC method, while the PSD obtained from the SAMWFMC method with the CFF becomes wider when decreasing C from 0.9 to 0.5.

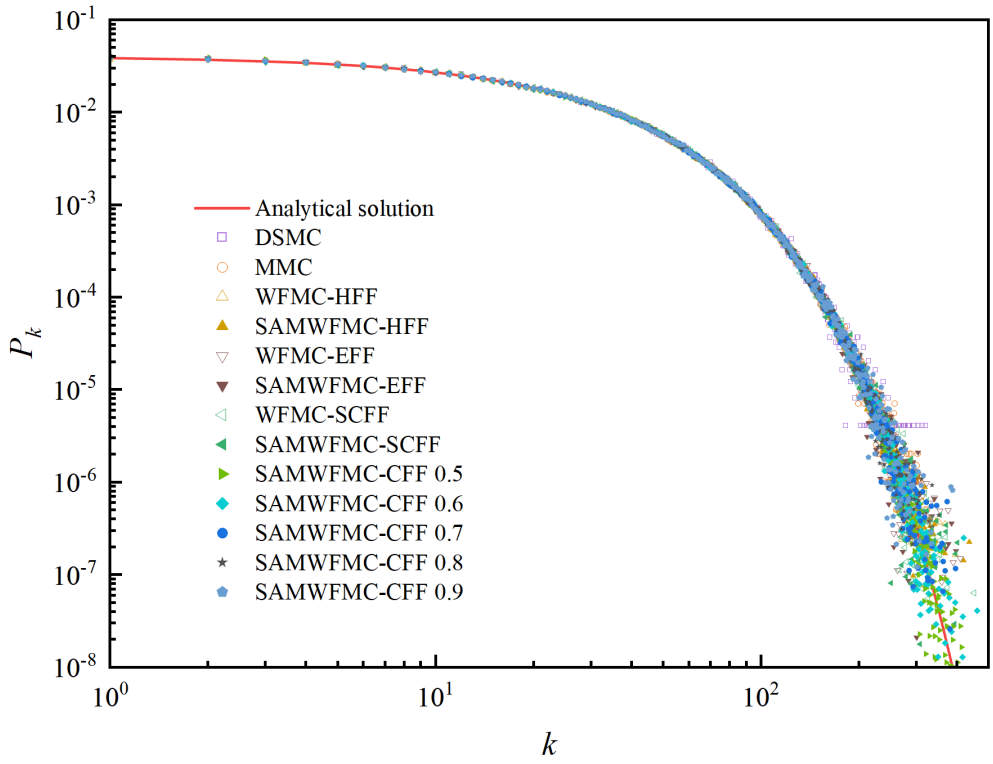

Figure 7 Probabilities of obtaining a cluster containing k primary particles, P_k obtained from DSMC, MMC, WFMC and SAMWFMC methods for different fraction functions with the IMD and CCK at $t/\tau_c = 50$ when compared with analytical solution.

Figure 8 shows the number of numerical particles, N_{NP} at different particle volumes, v/v_0 obtained from DSMC, MMC, WFMC and SAMWFMC methods for different fraction functions (i.e., HFF, EFF, SCFF and CFF) at $t/\tau_c = 50$. The DSMC method has the most numerical particles at $v/v_0 = 1$, but the number of numerical particles significantly reduces with the increase of the particle size. Finally, DSMC method has the least numerical particles at the high-end of the PSD, which implies that there are few or no numerical particles to represent the large real particles. This leads to the narrowest PSD among all MC methods, which is also shown in Figure 7, and the largest fluctuations in the high-order moments of the PSD (i.e., M_2 and M_3) are shown in Figures 6(c) and (d). By comparison, the MMC method distributes more numerical particles to represent the large real particles and extends the prediction of the PSD at the high-end, which reduces the fluctuations of M_2 and M_3 as shown in Figures 6(c) and (d). The number of numerical particles for the WFMC method for different fraction functions (i.e., HFF, EFF and SCFF) increases at first and then decreases with the increasing particle sizes, especially for the HFF, which is totally inconsistent with the DSMC and MMC methods. This implies that the WFMC

method changes the number distribution of the numerical particles, in which more numerical particles are used to represent larger real particles, but few numerical particles to represent smaller real particles. As a result, the WFMC method reduces the fluctuations in the high-order moments of the PSD (i.e. M_2 and M_3) as shown in Figures 6(c) and (d), but results in large fluctuation in the total number concentration, M_0 as shown in Figure 6(a), which is also found in the original work of Jiang and Chan (2021). The reason is that the statistic precision of stochastic approaches is inversely proportional to the square root of the numerical particle numbers. The SAMWFMC method for different fraction functions (i.e., HFF, EFF and SCFF) has the same trend as the MMC method in the number distribution of numerical particles, which decreases with the increase of the particle sizes. Compared with the WFMC method, more numerical particles at the low-end of the PSD but slightly less numerical particles at larger particle size areas are observed in the SAMWFMC method, therefore reducing the fluctuation in M_0 with less change in M_2 and M_3. In addition, it is found that the number distribution of numerical particles for the SAMWFMC method with the CFF gradually moves to the high-end of the PSD with the decrease of the constant, C from 0.9 to 0.5. It implies that the number of numerical particles with small sizes gradually decreases while the number of numerical particles with larger sizes increases, therefore resulting in the gradual reduction of the fluctuation in the high-order moments (i.e., M_2 and M_3) of the PSD as shown in Figures 6(c) and (d). It should be noted that the SAMWFMC method for the CFF ($C = 0.5$) has wider PSD and more numerical particles at $v/v_0 > 60$ than the WFMC method for the HFF, so smaller σ_{M_2} and σ_{M_3} for the former are shown in Figures 6(c) and (d). Although the PSD obtained from the SAMWFMC method for the CFF ($C = 0.7$) is almost as the same wide as the WFMC method for the HFF, the number of numerical particles for the former is less than that of the latter at $v/v_0 > 25$, leading to larger σ_{M_2} and σ_{M_3} for the former as shown in Figures 6(c) and (d).

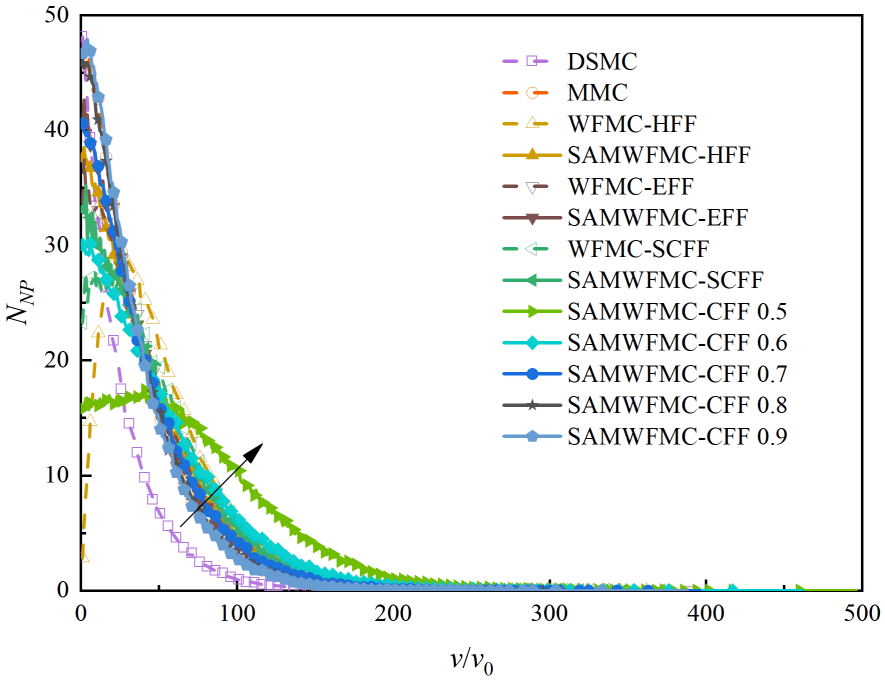

Figure 8 Number of numerical particles, N_{NP} at different particle volumes, v/v_0 obtained from DSMC, MMC, WFMC and SAMWFMC methods for different fraction functions with the IMD and CCK at $t/\tau_c = 50$.

3.2. Case 2: Initial monodispersed distribution and linear coagulation kernel function

The analytical solution of the Smoluchowski equation with the initial monodispersed distribution (IMD) and linear coagulation kernel (LCK) function is well known (Liffman, 1992), which is also used to validate the newly proposed SAMWFMC method. The initial total particle number concentration, $N_0 = 10^6$ particles/cm^3 (Kruis *et al.*, 2000) and the coagulation kernel $\beta_{ij} = A(v_i+v_j)$ where $A = 10^{-6}$ cm^3/s (Kruis *et al.*, 2000), v_i and v_j are the dimensionless volumes of the two coagulation particles, i and j, respectively. The characteristic coagulation time is defined as $\tau_c = 1/(AN_0)$. For simplicity, only the HFF for both WFMC and SAMWFMC methods and the CFF with C= 0.7 for the SAMWFMC method are used.

Figure 9 shows a very good agreement for zeroth-order to third-order moments (M_0, M_1, M_2 and M_3) between the analytical solutions (Liffman, 1992) and DSMC, MMC, WFMC and SAMWFMC methods for different fraction functions (i.e., HFF and CFF) with the IMD and LCK, and their corresponding mean standard deviations are also presented. All MC methods show an excellent mass/volume conservation, as the total volume/mass concentrations, M_1 for all MC methods remain

constant during the numerical simulation, therefore leading to no stochastic error in M_1 as shown in Figure 9(b). The mean standard deviations of zeroth-order to third-order moments (i.e., M_0, M_2 and M_3) obtained from different MC methods have a similar trend with time. The DSMC method has the largest σ_{M_0}, σ_{M_2} and σ_{M_3} among all MC methods. Although the σ_{M_2} and σ_{M_3} for the WFMC method are almost smaller than those of other MC methods, the WFMC method has larger σ_{M_0} than the MMC method but has just slightly smaller than the DSMC method. By comparison, the SAMWFMC method has the smallest σ_{M_0} among all MC methods and can achieve as low σ_{M_2} and σ_{M_3} as the WFMC method, which shows the advantage of the SAMWFMC method in reduction of the stochastic errors for M_0, M_2 and M_3, respectively. In addition, the SAMWFMC method for the CFF with $C = 0.7$ also has smaller σ_{M_0}, σ_{M_2} and σ_{M_3} than those of the DSMC and MMC methods, which demonstrates the newly proposed SAMWFMC method can deal with different fraction functions at very small stochastic error.

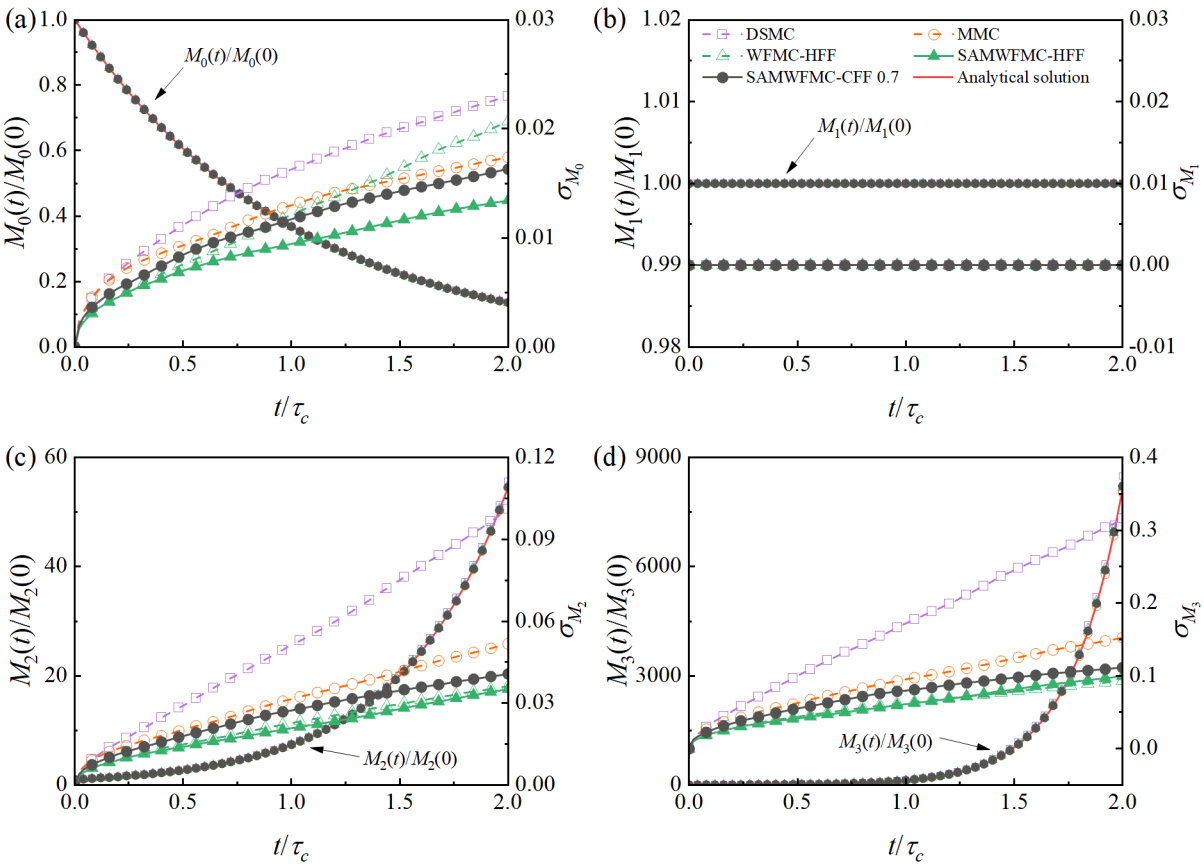

Figure 9 Time evolutions of zeroth-order to third-order moments (M_0, M_1, M_2 and M_3) and mean standard deviations obtained from DSMC, MMC, WFMC and SAMWFMC methods for different fraction functions with the IMD and LCK when compared with analytical solutions.

Figure 10 shows that the DSMC method has the narrowest particle size range and a slight wider particle size range with smaller fluctuation at the high-end is observed in the MMC method, which results in the differences of the σ_{M_2} and σ_{M_3} as shown in Figures 9(c) and 9(d), respectively. Compared with the MMC method, the fraction functions introduced in the WFMC and SAMWFMC methods can effectively extend the prediction of the particle size range and then obtain wider particle size ranges, which finally reduce the σ_{M_2} and σ_{M_3}. Small differences of σ_{M_2} and σ_{M_3} between the WFMC and SAMWFMC methods are found due to the almost identical width of particle size ranges.

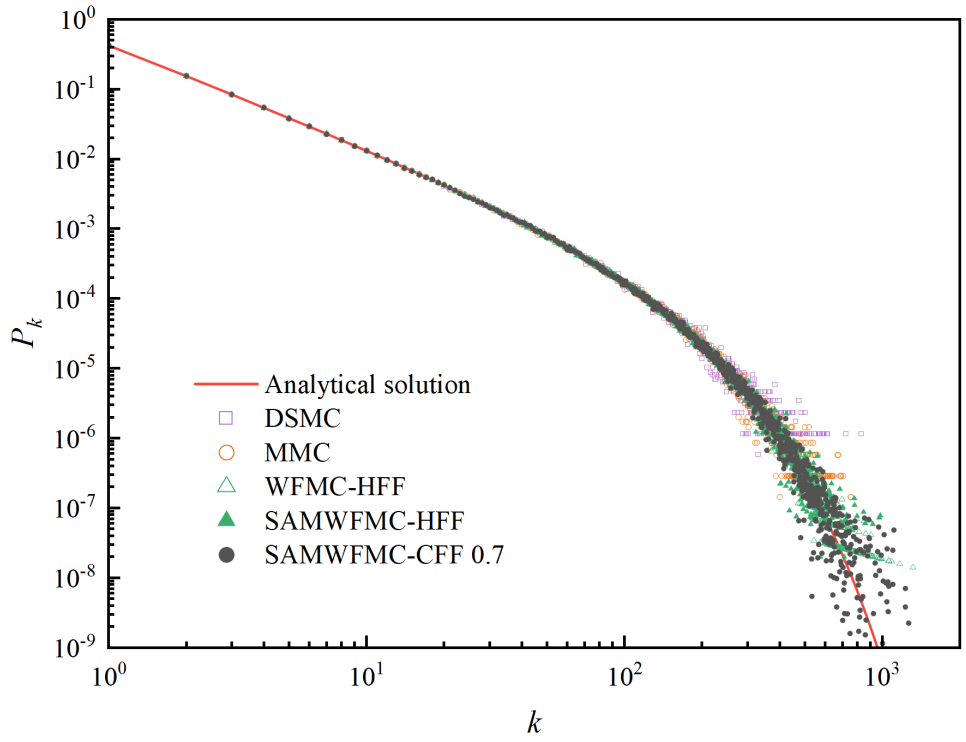

Figure 10 Probabilities of obtaining a cluster containing k primary particles, P_k obtained from DSMC, MMC, WFMC and SAMWFMC methods for different fraction functions with the IMD and LCK at $t/\tau_c = 2$ when compared with analytical solution.

3.3. Case 3: Initial monodispersed distribution and quadratic coagulation kernel function

Another benchmark test case with initial monodispersed distribution (IMD) and quadratic coagulation kernel (QCK) function is also validated in the present study, the analytical solution of this case exists in (Liffman, 1992). The initial total particle number concentration, $N_0 = 10^6$ particles/cm^3 (Kruis *et al.*, 2000) and the coagulation kernel, $\beta_{ij} = A(v_i \times v_j)$, where $A = 10^{-6}$ cm^3/s (Kruis *et al.*, 2000), v_i and v_j are the dimensionless volumes of a coagulation particle pair, i and j, respectively. The

characteristic coagulation time is defined as $\tau_c = 1/(AN_0)$. It should be noted that if the time is greater than τ_c, the analytical solution of the Smoluchowski equation does not exist (Kruis *et al.*, 2000) in this case due to the formation of the supercluster when $t = \tau_c$ (Liffman, 1992).

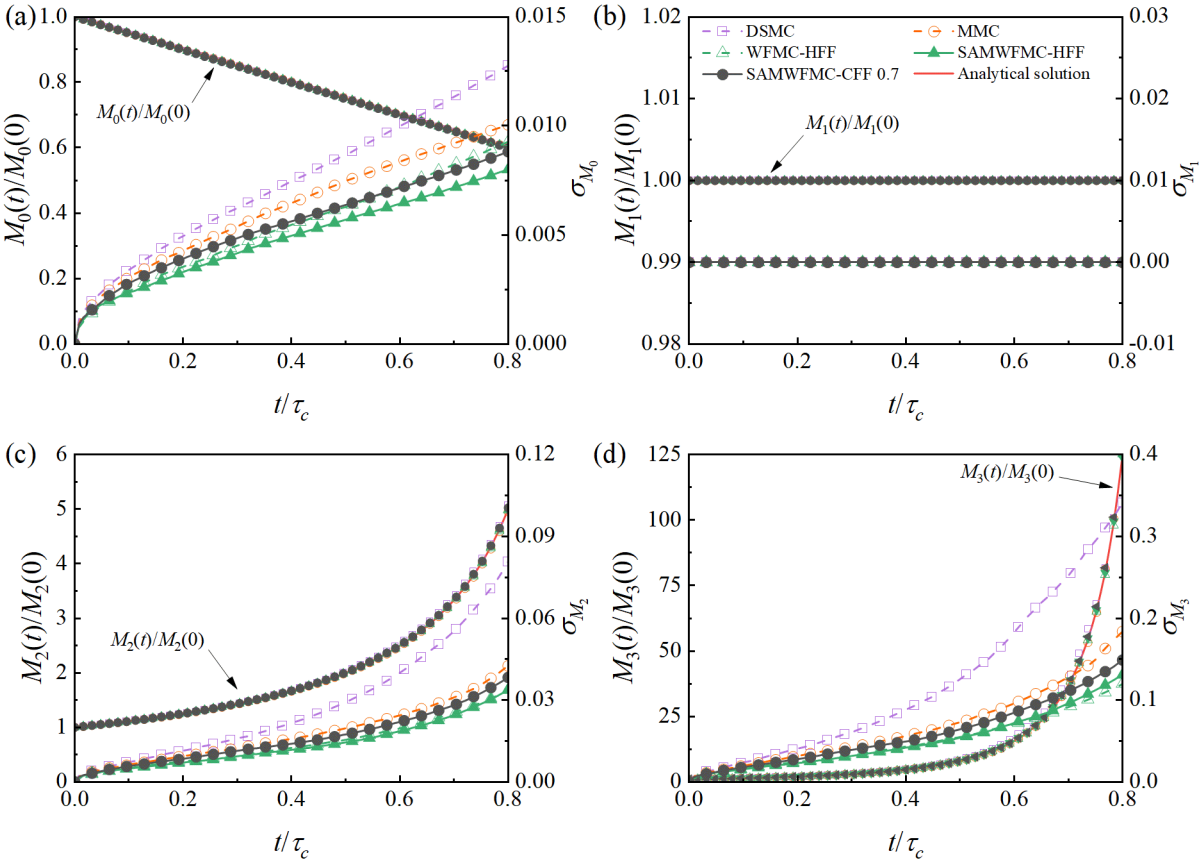

Figure 11 Time evolutions of zeroth-order to third-order moments and mean standard deviations for DSMC, MMC, WFMC and SAMWFMC methods for different fraction functions with the IMD and QCK when compared with analytical solutions.

Figures 11 and 12 are the time evolutions of zeroth-order to third-order moments and corresponding mean standard deviations and PSDs for different MC methods when compared with analytical solutions (Liffman, 1992), respectively. An excellent agreement of the first four moments for different MC methods and the analytical solutions with the IMD and QCK is observed in Figure 11. As the total volume/mass concentrations, M_1 for all MC methods remain constant, the resulting σ_{M_1} is always zero during the numerical simulation as shown in Figure 11(b). The SAMWFMC method has the lowest σ_{M_0} than other MC methods, while the σ_{M_2} and σ_{M_3} obtained from the SAMWFMC method are very close to those of the WFMC method because of the almost identical width of the PSDs as

shown in Figure 12, which are lower than those of the DSMC and MMC methods. This further demonstrates the contribution of the fraction functions to the PSD.

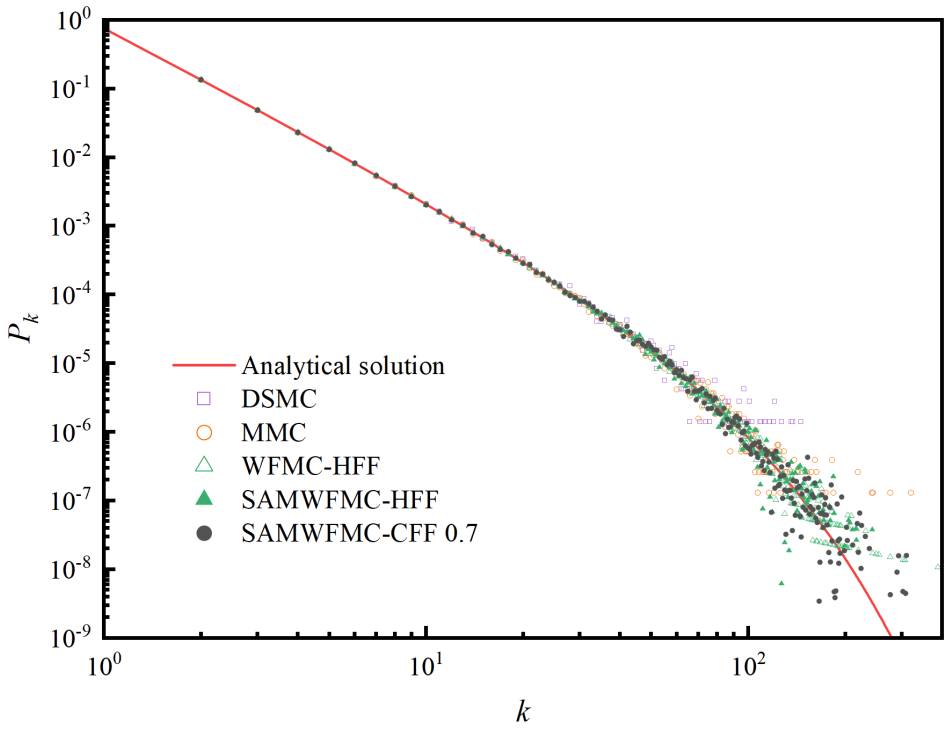

Figure 12 Probabilities of obtaining a cluster containing k primary particles, P_k obtained from DSMC, MMC, WFMC and SAMWFMC methods for different fraction functions with the IMD and QCK at t/τ_c= 0.8 when compared with analytical solution.

3.4. Case 4: Initial exponential distribution and constant coagulation kernel function

As particles with different sizes are more common than those with the same size in most practical cases involved in combustion emission sources and atmospheric aerosols (Friedlander, 2000), the newly proposed SAMWFMC method must be validated the computational accuracy with the initial polydisperse PSD. In the present study, an exponential function is chosen as the initial polydisperse PSD, which is given by (Zhao *et al.*, 2005b):

$$n_p(v,0)=N_0/v_0\,[\exp(-v/v_0)] \tag{25}$$

where N_0 is the initial total particle number concentration of real particles with the initial mean particle volume of v_0. The analytical solution of the Smoluchowski equation with the initial exponential distribution (IED) and constant coagulation kernel (CCK) function is provided in (Zhao *et al.*, 2005b). In the present study, N_0 = 10^6 particles/cm^3 (Zhao *et al.*, 2005b) and v_0 = 1 (dimensionless) are used.

The coagulation kernel, $\beta_{ij} = A$, where $A = 10^{-6}$ cm^3/s. The characteristic coagulation time is defined as $\tau_c = 1/(AN_0)$.

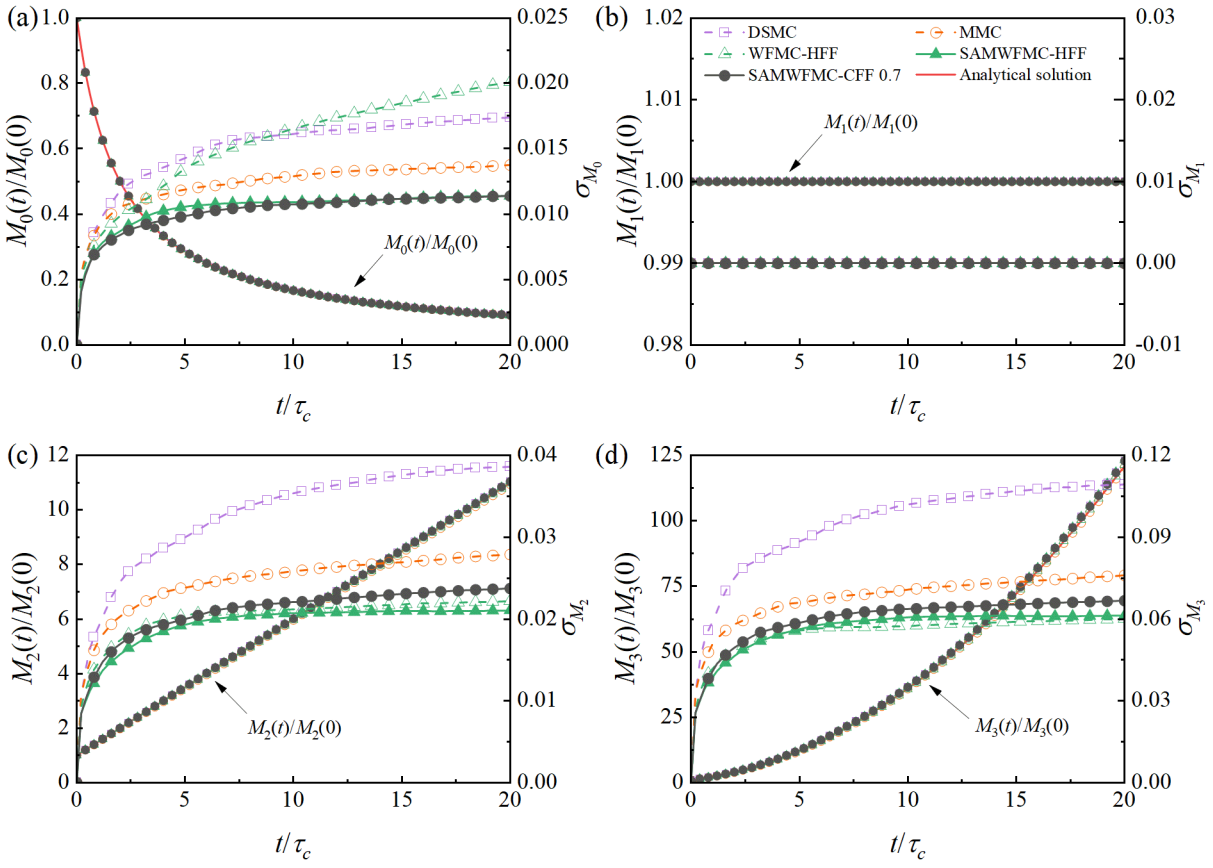

Figure 13 Time evolutions of zeroth-order to third-order moments and mean standard deviations obtained from DSMC, MMC, WFMC and SAMWFMC methods for different fraction functions with the IED and CCK when compared with analytical solutions.

A very good agreement between the analytical solutions (Zhao *et al.*, 2005b) and the first four moments (i.e., M_0, M_1, M_2 and M_3) obtained from different MC methods (i.e., DSMC, MMC, WFMC and SAMWFMC) for different fraction functions (i.e., HFF and CFF) with the IED and CCK is shown in Figure 13. The results of M_1 obtained from the four MC methods remain constant and there are no changes in σ_{M_1} for all MC methods during the numerical simulation as shown in Figure 13(b). The SAMWFMC method with the HFF and CFF has the lowest σ_{M_0}, while the WFMC method has the largest σ_{M_0} among all MC methods, which is even larger than that of the DSMC method and keeps increasing with time. With the HFF, the σ_{M_2} and σ_{M_3} for the SAMWFMC and WFMC methods are very close to each other and have the lowest stochastic errors. It demonstrates that the SAMWFMC method can

achieve lower stochastic error in M_0 and nearly the equally lowest stochastic errors in M_2 and M_3, respectively when compared with the WFMC method. It also implies that the SAMWFMC method surpass the WFMC method in obtaining accurate numerical results. In addition, the SAMWFMC method with CFF has lower σ_{M_0}, σ_{M_2} and σ_{M_3} than the MMC and DSMC methods, which also demonstrates the significant improvement in computational accuracy by the SAMWFMC method.

Figure 14 shows the dimensionless particle number concentration (PNC) functions at different particle volumes, v/v_0 obtained from DSMC, MMC, WFMC and SAMWFMC methods for different fraction functions (i.e., HFF and CFF) with the IED and CCK at $t/\tau_c = 0$, 1, 5 and 20 when compared with analytical solutions (Zhao *et al.*, 2005b). In here, $t/\tau_c = 0$ is the initial particle number concentration function. A very good agreement between the analytical solutions and the numerical results obtained from different MC methods is observed at different times, t/τ_c. As coagulation events take place, particle sizes become larger with time and the PNC functions gradually moves to the right side, but the PNC functions still remain the "self-preserving" form (Friedlander, 2000). It is still shown that the WFMC and SAMWFMC methods can obtain particles with larger volumes than the DSMC and MMC methods, and also extend the prediction of the particle volumes at the high-end. It also implies that the introduction of the fraction functions can significantly reduce the σ_{M_2} and σ_{M_3} in the MC simulations with initial polydispersed distribution. The particle size range obtained from the MMC method are slightly wider than that of the DSMC method, which leads to the differences in the stochastic errors of the high-order moments in Figures 13(c) and (d). The large particle size regime for the WFMC and SAMWFMC methods are almost identical at $t/\tau_c = 1$, but the difference becomes larger with time. The WFMC method can obtain larger particles at the high-end than the SAMWFMC method when $t/\tau_c = 20$, and the volume of particles at the low-end for the WFMC method is also larger than those of all the MC methods. It further demonstrates that the WFMC method is developed to obtain more particles with large volumes, in which smaller real particles are poorly or even not represented. As a result, the WFMC method achieves very low σ_{M_3} as shown in Figures 13(d) by the contribution of those large volume particles but deteriorates the statistical precision at the low-end. By comparison, although the volume of particles obtained from the SAMWFMC method at the high-end is smaller, the small particles at the

low-end is still represented, which lead to slightly larger σ_{M_3} and even lower σ_{M_2}, but significantly lower σ_{M_0} as shown in Figures 13(c), 13(d) and 13(a), respectively. As the volume/mass is always conserved during numerical simulation, the σ_{M_1} for both WFMC and SAMWFMC methods are equal to zero as shown in Figure 13(b).

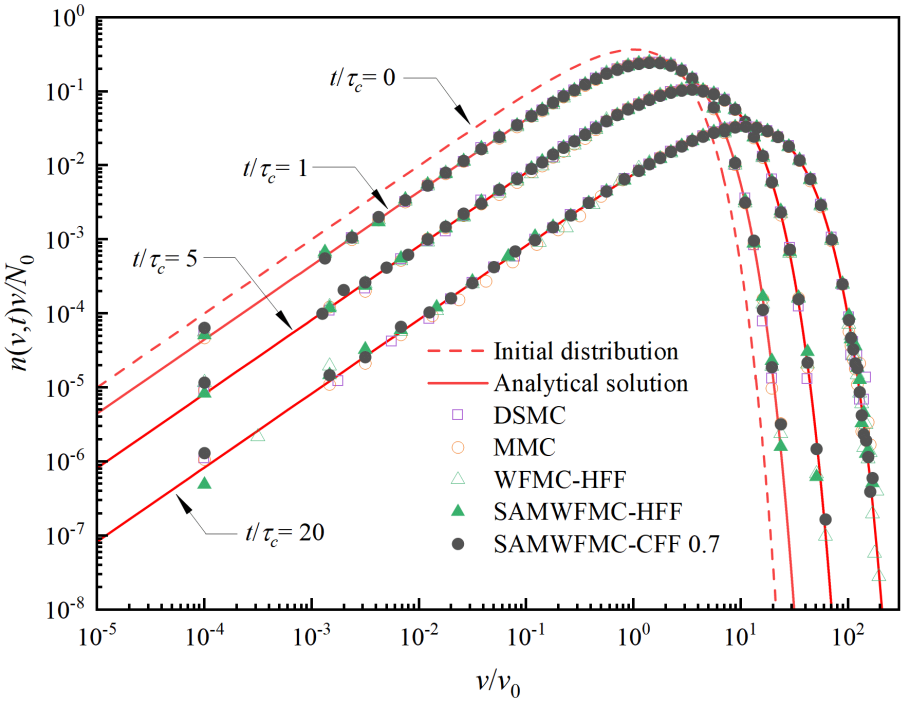

Figure 14 Dimensionless particle number concentration functions at different particle volumes, v/v_0 obtained from DSMC, MMC, WFMC and SAMWFMC methods for different fraction functions with the IED and CCK at t/τ_c=0, 1, 5 and 20 when compared with analytical solutions.

3.5. Case 5: Initial exponential distribution and linear coagulation kernel function

There also exists the analytical solution of the Smoluchowski equation with the initial exponential distribution (IED) and linear coagulation kernel (LCK) function in (Zhao *et al.*, 2005b). In the present study, $N_0 = 10^6$ particles/cm^3 (Zhao *et al.*, 2005b) and $v_0 = 1$ (dimensionless) are used. The coagulation kernel, $\beta_{ij} = A(v_i+v_j)$, where $A = 10^{-6}$ cm^3/s, v_i and v_j are the dimensionless volumes of the two coagulation particles, i and j, respectively. The characteristic coagulation time is defined as $\tau_c = 1/(AN_0v_0)$.

Figure 15 shows the time evolutions of first four moments (i.e., M_0, M_1, M_2 and M_3) obtained from different MC methods and corresponding mean standard deviations (i.e., σ_{M_0}, σ_{M_1}, σ_{M_2} and σ_{M_3})

for different fraction functions (i.e., HFF and CFF) with the IED and LCK when compared with analytical solutions (Zhao *et al.*, 2005b). The first four moments for all MC methods have a very good agreement with the analytical solutions. The SAMWFMC method with the CFF has the lowest σ_{M_0}, while the σ_{M_0} for the DSMC method is the largest. The stochastic error in M_0 introduced by the WFMC method is still larger than that of the MMC method, but the SAMWFMC method with HFF has lower σ_{M_0} than the MMC method. The σ_{M_2} and σ_{M_3} for the SAMWFMC and WFMC methods with different fraction functions (i.e., HFF and CFF) are very close to each other but are smaller than those of the DSMC and MMC methods. There are no changes in σ_{M_1} for all MC methods as shown in Figure 15(b) since the volume/mass is always conserved during the numerical simulation.

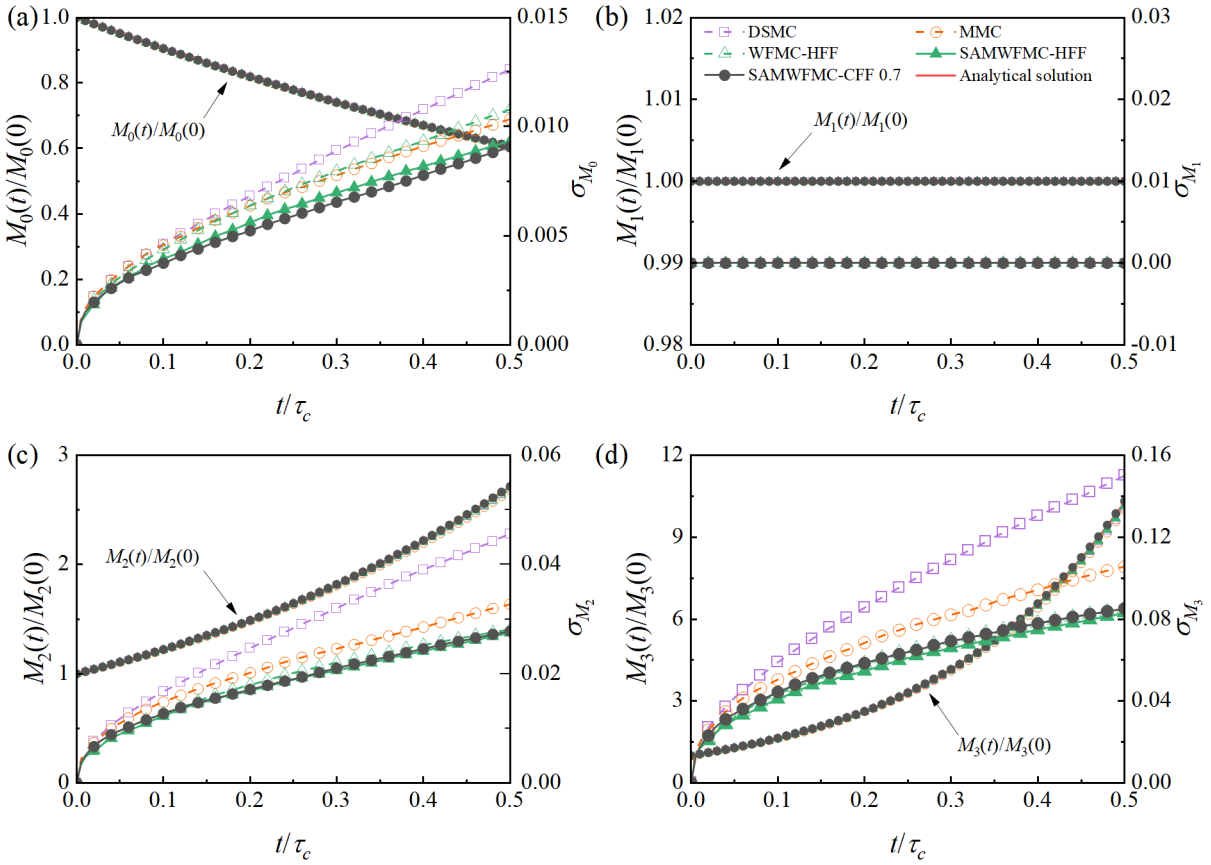

Figure 15 Time evolutions of zeroth-order to third-order moments and mean standard deviations obtained from DSMC, MMC, WFMC and SAMWFMC methods for different fraction functions with the IED and LCK when compared with analytical solutions.

Figure 16 shows the dimensionless PNC functions at different particle volumes, v/v_0 for different MC methods for different fraction functions with the IED and LCK at $t/\tau_c = 0$ and 0.5 when compared

with the analytical solution (Zhao *et al.*, 2005b). In here, t/τ_c = 0 is the initial particle number concentration function. The numerical results obtained from DSMC, MMC, WFMC and SAMWFMC methods have an excellent agreement with the analytical solution. The DSMC method has narrower particle size range than other MC methods while the particle size range for the MMC method is obviously wider due to the introduction of the weight numerical particles. Compared with the DSMC and MMC methods, the WFMC and SAMWFMC methods have wider particle size ranges due to the occurrence of the larger size particles at the high-end, which have been proved to have contribution to the high-order moments.

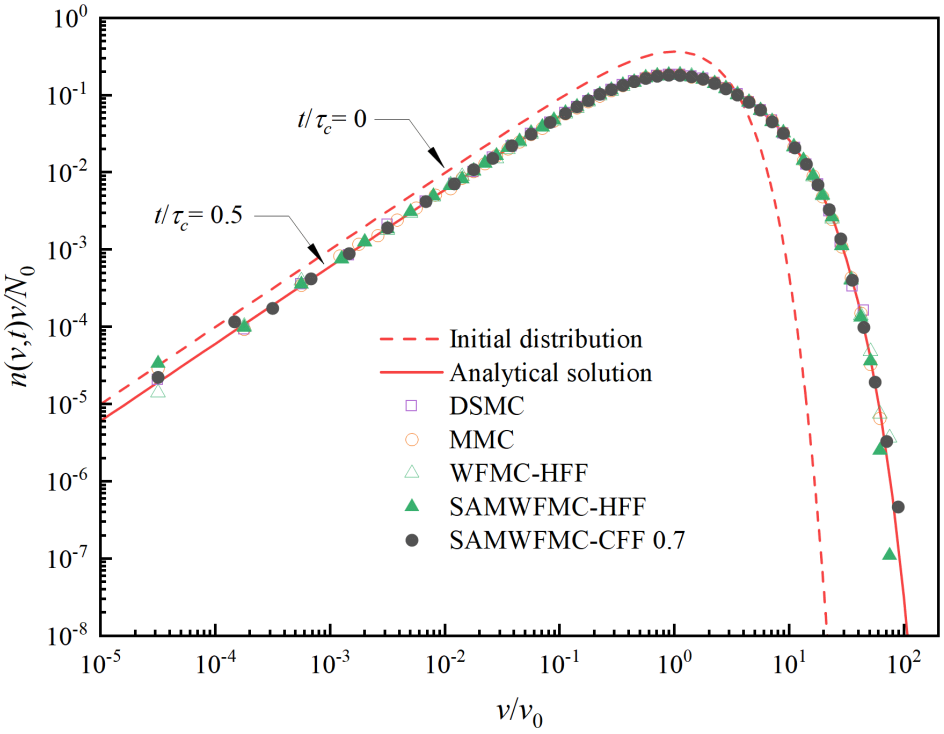

Figure 16 Dimensionless particle number concentration functions at different particle volumes, v/v_0 obtained from DSMC, MMC, WFMC and SAMWFMC methods for different fraction functions with the IED and LCK at t/τ_c= 0.5 when compared with analytical solution.

3.6. Case 6: Initial exponential distribution and quadratic coagulation kernel function

The initial exponential distribution (IED) and quadratic coagulation kernel (QCK) function are also used to validate the computational accuracy of the SAMWFMC method when compared with the analytical solution (Zhao *et al.*, 2005b). In this case, $N_0 = 10^6$ particles/cm^3 (Zhao *et al.*, 2005b) and v_0 = 1 (dimensionless) are used. The coagulation kernel, $\beta_{ij} = A(v_i \times v_j)$, where $A = 10^{-6}$ cm^3/s, v_i and v_j are the dimensionless volumes of the two coagulation particles, i and j, respectively. The characteristic

coagulation time is defined as $\tau_c = 1/(AN_0v_0^2)$. It is reported that the critical phenomena of gelation may be caused by the quadratic coagulation kernel in this case, but the existing analytical solution is still useful for the algorithm validation (Zhao *et al.*, 2005b).

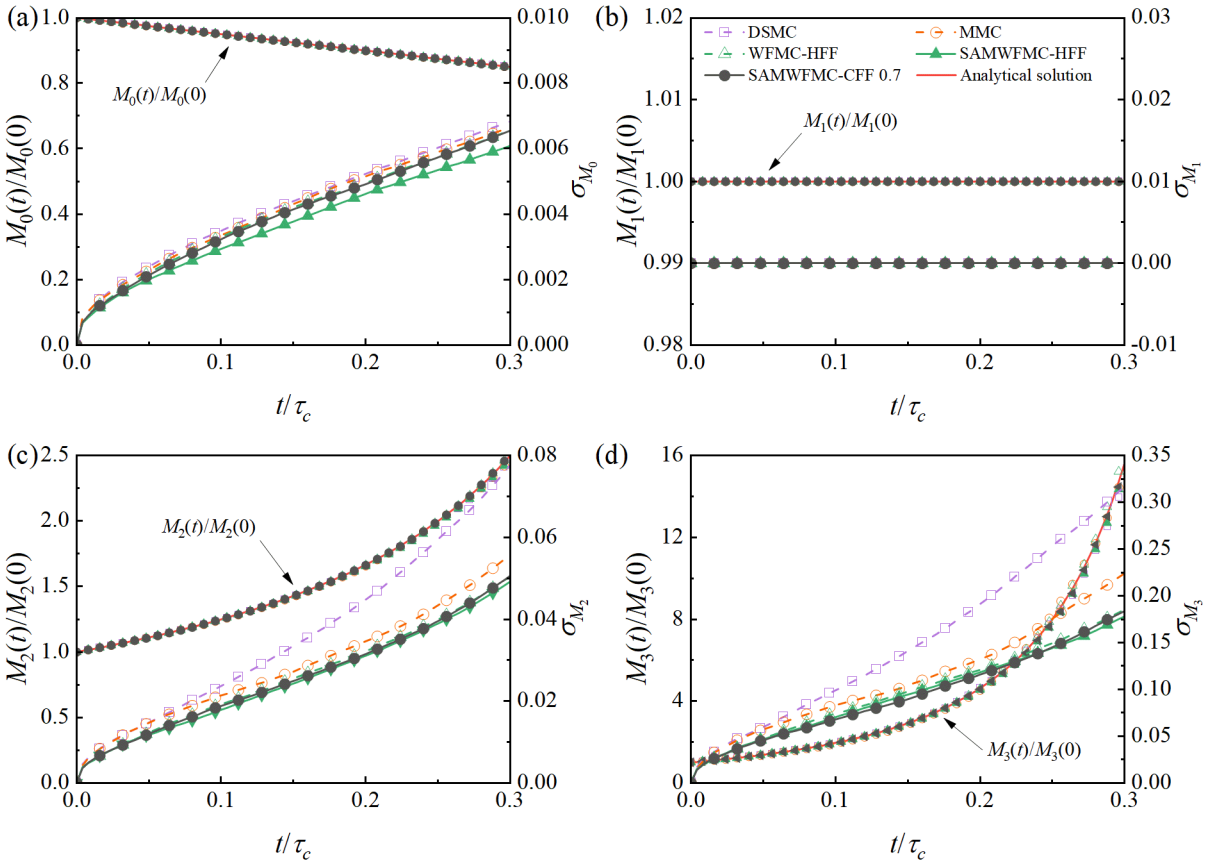

Figure 17 Time evolutions of zeroth-order to third-order moments and mean standard deviations obtained from DSMC, MMC, WFMC and SAMWFMC methods for different fraction functions with the IED and QCK when compared with analytical solutions.

Figure 17 shows that the time evolutions of first four moments (i.e., M_0, M_1, M_2 and M_3) obtained from different MC methods (i.e., DSMC, MMC, WFMC and SAMWFMC) have a very good agreement with analytical solutions (Zhao *et al.*, 2005b). The results of M_1 and σ_{M_1} obtained from all MC methods remain constant during the numerical simulation as shown in Figure 17(b). The SAMWFMC method has smaller σ_{M_0}, σ_{M_2} and σ_{M_3} than other MC methods. A very good agreement of the PNC functions at different particle volumes, v/v_0 between the analytical solution and numerical results for all MC methods is also found at t/τ_c= 0.3 in Figure 18, but the differences among these MC methods are also clear. The particle size ranges obtained from the WFMC and SAMWFMC methods are still found to be wider than

those of the DSMC and MMC methods, which leads to lower stochastic errors in the high-order moments. This further demonstrates the significant effect of the fraction functions on the computational accuracy in the high-order moments.

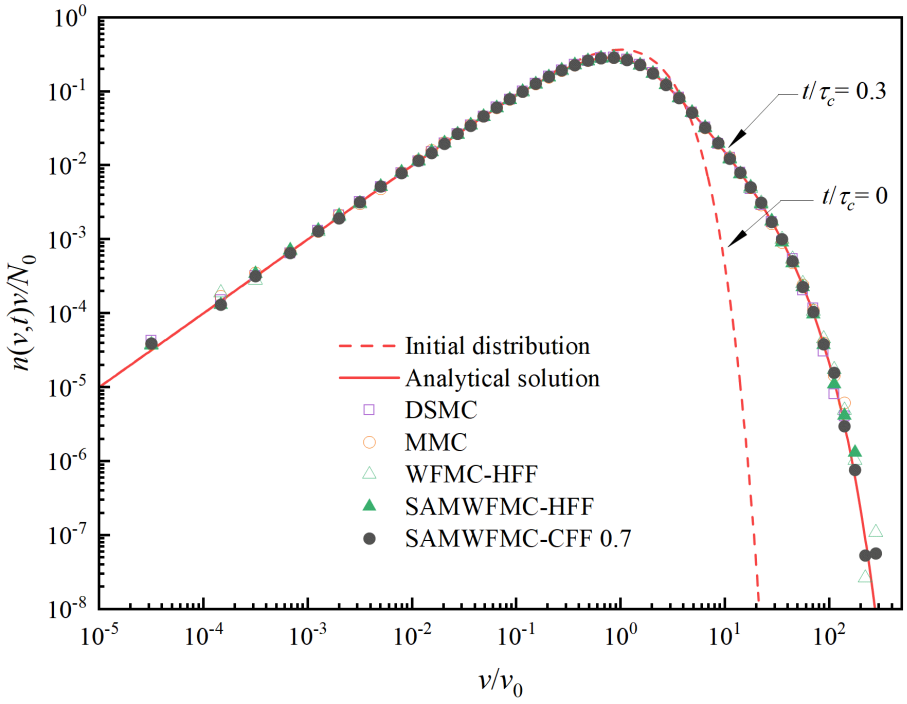

Figure 18 Dimensionless particle number concentration functions at different particle volumes, v/v_0 obtained from DSMC, MMC, WFMC and SAMWFMC methods for different fraction functions with the IED and QCK at $t/\tau_c = 0.3$ when compared with analytical solution.

3.7. Computational efficiency

The computational efficiency of the new SAMWFMC method is evaluated by comparing with other studied MC methods. The computational time required for the WFMC method with the HFF in each case is regarded as the reference time because the WFMC method with the HFF has been fully tested for different cases in Jiang and Chan (2021) and also used for studying soot aerosol dynamics in Jiang and Chan (2022). Hence, the corresponding normalized computational times of different cases required for all MC methods are listed in Table 1.

Table 1 Normalized computational times of different cases for all studied MC methods.

Case	DSMC	MMC	WFMC		SAMWFMC		SAMWFMC	
1	0.21	0.65	HFF EFF SCFF	1 1.00 1.72	HFF EFF SCFF	1.40 1.44 2.51	CFF 0.5 CFF 0.6 CFF 0.7 CFF 0.8 CFF 0.9	2.82 2.14 1.83 1.50 1.39
2	0.07	0.45	HFF	1	HFF	1.01	CFF 0.7	1.49
3	0.17	0.55	HFF	1	HFF	1.19	CFF 0.7	1.32
4	0.22	0.63	HFF	1	HFF	1.39	CFF 0.7	1.83
5	0.25	0.62	HFF	1	HFF	1.25	CFF 0.7	1.69
6	0.30	0.64	HFF	1	HFF	1.22	CFF 0.7	1.47

Results show that the computational times required for the DSMC method are the lowest among all MC methods, the reason is that when the DSMC method is used, the number of numerical particles gradually reduces with time due to the occurrence of coagulation events, which lowers the computational cost. However, the decrease in the number of numerical particles has a significant adverse effect on the computational accuracy. The MMC, WFMC and SAMWFMC methods remain the number of numerical particles unchanged during the numerical simulation which can improve the computational accuracy but it definitely leads to larger consumption of computational times. As the introduction of fraction functions to the WFMC and SAMWFMC methods leads to larger C_{ij} in Equation 5 and C_0 in Equation 7 but has smaller time step, Δt in Equation 9 than those of the MMC method, therefore requiring more computational times. When the fraction function (i.e., HFF, EFF or SCFF) is the same, the computational times for the SAMWFMC method are slightly longer than those of the WFMC method in each case. The reason is that when compared with the WFMC method, the central processing units (CPUs) require more computational cost to deal with the operations of sorting and merging numerical particles in the SAMWFMC method. The computational cost required by Case 1 with and without insertion sort is also evaluated. It is worth noting that if the sorting algorithm (i.e., insertion sort) is not used, then a very large statistical noise is obtained and the computational accuracy is largely reduced. Hence, only the computational efficiency is discussed here. Numerical results show that the computational cost for sorting numerical particles is 1.05 times of that without having insertion sort. It implies that the insertion sort is highly computational efficient when dealing with nearly sorted arrays. Hence, the finding and merging numerical particles require a slightly more computational cost

in the SAMWFMC method when compared with the removing operation in the WFMC method. However, considering the high computational accuracy in high-order moments and significant reduction in the stochastic error in the particle number concentration, the computational cost of the SAMWFMC method is highly acceptable. In addition, the computational time for the SAMWFMC method with the CFF significantly reduces when the constant C increases from 0.5 to 0.9, the reason is that the C_{ij} in Equation 5 and C_0 in Equation 7 become smaller while the time step, Δt in Equation 9 becomes larger. As the stochastic errors in different moments (i.e., M_0, M_2 and M_3) are very low and the stochastic errors in M_1 are always zero due to volume/mass conservation for the SAMWFMC method for the CFF with C = 0.5 to 0.9, the choice of the constant, C is mainly dependent on the computational cost.

4. Conclusions

A new Monte Carlo method based on sorting algorithm is proposed and developed for solving the weighted fraction coagulation process in aerosol dynamics. In the new sorting algorithm-based merging weighted fraction Monte Carlo (SAMWFMC) method, three types of fraction functions (HFF, EFF and SCFF) are used to validate the computational accuracy and efficiency. Constant fraction functions are not applicable to the WFMC method but are also introduced to extend the generality of the fraction functions and used to evaluate the reliability of the newly developed SAMWFMC method. A new merging weighted fraction scheme is also proposed to ensure that the number of numerical particles and the volume of computational domain are constant. Six benchmark test cases are used to fully validate the SAMWFMC method by comparing with the existing analytical solutions as well as the numerical results of the direct simulation Monte Carlo (DSMC), multi-Monte Carlo (MMC) and weighted fraction Monte Carlo (WFMC) methods. The main conclusions are drawn as follows:

1. The particle number concentration (PNC) function and the zeroth-order to third-order moments (i.e., M_0, M_1, M_2 and M_3) obtained from the SAMWFMC method show excellent agreement with analytical solutions. As M_1 for all MC methods remain constant, their corresponding stochastic errors are always zero during the numerical simulation.

2. The SAMWFMC method has lower stochastic errors in M_0, M_2 and M_3 than the DSMC and MMC

methods. Compared with the WFMC method, the SAMWFMC method does not increase the stochastic errors in high-order moments (i.e., M_2 and M_3) but significantly reduces the stochastic error in the total particle number concentration, M_0, even though the computational cost of the new SAMWFMC method is slightly higher than that of the WFMC method. Furthermore, the numerical results obtained from the SAMWFMC method with constant fraction functions show excellent agreement with analytical solutions with very low stochastic errors in M_0, M_2 and M_3 and no stochastic error in M_1.

3. The new SAMWFMC method shows a significant advantage in dealing with weighted fraction coagulation process in aerosol dynamics. It also demonstrates that the SAMWFMC method provides excellent potential to deal with various fraction functions with high computational accuracy and efficiency.

Acknowledgements

Will be filled in the information of funding bodies and institutions due to this journal policy of anonymous reviewing process in the early stage.

References

Chan, T.L., Liu, S.Y. and Yue, Y. (2018), "Nanoparticle formation and growth in turbulent flows using the bimodal TEMOM", *Powder Technology*, Vol. 323, pp. 507-517.

Cook, C.R. and Kim, D.J. (1980), "Best sorting algorithm for nearly sorted lists", *Communications of the ACM*, Vol. 23 No. 11, pp. 620-624.

Debry, E., Sportisse, B. and Jourdain, B. (2003), "A stochastic approach for the numerical simulation of the general dynamics equation for aerosols", *Journal of Computational Physics*, Vol. 184 No. 2, pp. 649-669.

Deville, R.E.L., Riemer, N. and West, M. (2011), "Weighted Flow Algorithms (WFA) for stochastic particle coagulation", *Journal of Computational Physics*, Vol. 230 No. 23, pp. 8427-8451.

Frenklach, M. and Harris, S.J. (1987), "Aerosol dynamics modeling using the method of moments", *Journal of Colloid and Interface Science*, Vol. 118 No. 1, pp. 252-261.

Friedlander, S.K. (2000), *Smoke, Dust, and Haze: Fundamentals of Aerosol Dynamics*, Oxford University Press, New York.

Garcia, A.L., Broeck, C.V.D., Aertsens, M. and Serneels, R. (1987), "A Monte Carlo simulation of coagulation", *Physica A: Statistical Mechanics and its Applications*, Vol. 143, pp. 535-546.

Gelbard, F., Tambour, Y. and Seinfeld, J.H. (1980), "Sectional representations for simulating aerosol dynamics", *Journal of Colloid and Interface Science*, Vol. 76 No. 2, pp. 541-556.

Gillespie, D.T. (1975), "An exact method for numerically simulating the stochastic coalescence process in a cloud", *Journal of the Atmospheric Sciences*, Vol. 32 No. 10, pp. 1977-1989.

Goel, S. and Kumar, R. (2018), "Brownian Motus and Clustered Binary insertion sort methods: An efficient progress over traditional methods", *Future Generation Computer Systems*, Vol. 86, pp. 266-280.

Jiang, H., Yu, M.Z., Shen, J. and Xie, M. (2021), "Inverse Gaussian distributed method of moments for agglomerate coagulation due to Brownian motion in the entire size regime", *International Journal of Heat and Mass Transfer*, Vol. 173, Article ID 121229, 10 pages.

Jiang, X. and Chan, T.L. (2021), "A new weighted fraction Monte Carlo method for particle coagulation", *International Journal of Numerical Methods for Heat & Fluid Flow*, Vol. 31 No. 9, pp. 3009-3029.

Jiang, X. and Chan, T.L. (2022), "Lagrangian particle tracking with new weighted fraction Monte Carlo method for studying the soot particle size distributions in premixed flames", *International Journal of Numerical Methods for Heat & Fluid Flow*, Vol. 32 No. 6, pp. 1961-1998.

Kapur, E., Kumar, P. and Gupta, S. (2012), "Proposal of a two way sorting algorithm and performance comparison with existing algorithms", *International Journal of Computer Science, Engineering and Applications*, Vol. 2, pp. 61-78.

Kotalczyk, G. and Kruis, F.E. (2017), "A Monte Carlo method for the simulation of coagulation and nucleation based on weighted particles and the concepts of stochastic resolution and merging", *Journal of Computational Physics*, Vol. 340, pp. 276-296.

Kruis, F.E., Maisels, A. and Fissan, H. (2000), "Direct simulation Monte Carlo method for particle coagulation and aggregation", *AIChE Journal*, Vol. 46 No. 9, pp. 1735-1742.

Kruis, F.E., Wei, J., Van Der Zwaag, T. and Haep, S. (2012), "Computational fluid dynamics based stochastic aerosol modeling: Combination of a cell-based weighted random walk method and a constant-number Monte-Carlo method for aerosol dynamics", *Chemical Engineering Science*, Vol. 70, pp. 109-120.

Li, D., Li, Z. and Gao, Z. (2019), "Quadrature-based moment methods for the population balance equation: An algorithm review", *Chinese Journal of Chemical Engineering*, Vol. 27 No. 3, pp. 483-500.

Liffman, K. (1992), "A direct simulation Monte-Carlo method for cluster coagulation", *Journal of Computational Physics*, Vol. 100 No. 1, pp. 116-127.

Lin, Y., Lee, K. and Matsoukas, T. (2002), "Solution of the population balance equation using constant-number Monte Carlo", *Chemical Engineering Science*, Vol. 57 No. 12, pp. 2241-2252.

Liu, H.M. and Chan, T.L. (2018a), "Differentially weighted operator splitting Monte Carlo method for simulating complex aerosol dynamic processes", *Particuology*, Vol. 36, pp. 114-126.

Liu, H.M. and Chan, T.L. (2018b), "Two-component aerosol dynamic simulation using differentially weighted operator splitting Monte Carlo method", *Applied Mathematical Modelling*, Vol. 62, pp. 237-253.

Liu, H.M. and Chan, T.L. (2020), "A coupled LES-Monte Carlo method for simulating aerosol dynamics in a turbulent planar jet", *International Journal of Numerical Methods for Heat & Fluid Flow*, Vol. 30 No. 2, pp. 855-881.

Liu, H.M., Jiang, W., Liu, W., Liu, X., Liu, S.Y. and Chan, T.L. (2021), "Monte Carlo simulation of polydisperse particle deposition and coagulation dynamics in enclosed chambers", *Vacuum*, Vol. 184, Article ID 109952, 11 pages.

Liu, H., Shao, J., Jiang, W. and Liu, X. (2022), "Numerical modeling of droplet aerosol coagulation, condensation/evaporation and deposition processes", *Atmosphere*, Vol. 13 No. 2, Article ID 326, 15 pages.

Liu, S.Y. and Chan, T.L. (2017), "A stochastically weighted operator splitting Monte Carlo (SWOSMC) method for the numerical simulation of complex aerosol dynamic processes", *International Journal of Numerical Methods for Heat & Fluid Flow*, Vol. 27 No. 1, pp. 263-278.

Liu, S.Y., Chan, T.L., He, Z., Lu, Y.Y., Jiang, X. and Wei, F.Z. (2019a), "Soot formation and evolution characteristics in premixed methane/ethylene-oxygen-argon burner-stabilized stagnation flames", *Fuel*, Vol. 242, pp. 871-882.

Liu, S.Y., Chan, T.L., Lin, J.Z. and Yu, M.Z. (2019b), "Numerical study on fractal-like soot aggregate dynamics of turbulent ethylene-oxygen flame", *Fuel*, Vol. 256, pp. 115857, 21 pages.

Liu, S.Y., Chan, T.L. and Liu, H.J. (2019c), "Numerical simulation of particle formation and evolution in a vehicle exhaust plume using the bimodal Taylor expansion method of moments", *Particuology*, Vol. 43, pp. 46-55.

Mcgraw, R. (1997), "Description of aerosol dynamics by the Quadrature Method of Moments", *Aerosol Science and Technology*, Vol. 27 No. 2, pp. 255-265.

Prakash, A., Bapat, A.P. and Zachariah, M.R. (2003), "A simple numerical algorithm and software for solution of nucleation, surface growth, and coagulation problems", *Aerosol Science and Technology*, Vol. 37 No. 11, pp. 892-898.

Ramabhadran, T.E., Peterson, T.W. and Seinfeld, J.H. (1976), "Dynamics of aerosol coagulation and condensation", *AIChE Journal*, Vol. 22 No. 5, pp. 840-851.

Sedgewick, R. and Wayne, K. (2011), *Algorithms*, Addison-Wesley, Upper Saddle River, NJ.

Shen, J., Jiang, H., Yu, M.Z. and Kong, B. (2022), "A bimodal population balance method for the dynamic process of engineered nanoparticles", *International Journal of Heat and Mass Transfer*, Vol. 188, Article ID 122605, 14 pages.

Shen, J., Yu, M.Z., Chan, T.L., Tu, C. and Liu, Y. (2020), "Efficient method of moments for simulating atmospheric aerosol growth: Model description, verification, and application", *Journal of Geophysical Research: Atmospheres*, Vol. 125 No. 13, Article ID e2019JD032172, 22 pages.

Smith, M. and Matsoukas, T. (1998), "Constant-number Monte Carlo simulation of population balances", *Chemical Engineering Science*, Vol. 53 No. 9, pp. 1777-1786.

Wang, K., Yu, S. and Peng, W. (2020), "An analytical solution of the population balance equation for simultaneous Brownian and shear coagulation in the continuum regime", *Advanced Powder Technology*, Vol. 31 No. 5, pp. 2128-2135.

Wu, S., Yang, S., Tay, K.L., Yang, W. and Jia, M. (2022), "A hybrid sectional moment projection method for discrete population balance dynamics involving inception, growth, coagulation and fragmentation", *Chemical Engineering Science*, Vol. 249, Article ID 117333, 17 pages.

Xu, Z., Zhao, H. and Zheng, C. (2014), "Fast Monte Carlo simulation for particle coagulation in population balance", *Journal of Aerosol Science*, Vol. 74, pp. 11-25.

Xu, Z., Zhao, H. and Zheng, C. (2015), "Accelerating population balance-Monte Carlo simulation for coagulation dynamics from the Markov jump model, stochastic algorithm and GPU parallel computing", *Journal of Computational Physics*, Vol. 281, pp. 844-863.

Yang, H., Lin, J.Z. and Chan, T.L. (2020), "Effect of fluctuating aerosol concentration on the aerosol distributions in a turbulent jet", *Aerosol and Air Quality Research*, Vol. 20, pp. 1629-1639.

Yu, M.Z. and Chan, T.L. (2015), "A bimodal moment method model for submicron fractal-like agglomerates undergoing Brownian coagulation", *Journal of Aerosol Science*, Vol. 88, pp. 19-34.

Yu, M.Z., Lin, J.Z. and Chan, T.L. (2008), "A new moment method for solving the coagulation equation for particles in Brownian motion", *Aerosol Science and Technology*, Vol. 42 No. 9, pp. 705-713.

Zhang, H., Sharma, G., Dhawan, S., Dhanraj, D., Li, Z. and Biswas, P. (2020), "Comparison of discrete, discrete-sectional, modal and moment models for aerosol dynamics simulations", *Aerosol Science and Technology*, Vol. 54 No. 7, pp. 739-760.

Zhao, H., Kruis, F.E. and Zheng, C. (2009), "Reducing statistical noise and extending the size spectrum by applying weighted simulation particles in Monte Carlo simulation of coagulation", *Aerosol Science and Technology*, Vol. 43 No. 8, pp. 781-793.

Zhao, H. and Zheng, C. (2009a), "Correcting the multi-Monte Carlo method for particle coagulation", *Powder Technology*, Vol. 193 No. 1, pp. 120-123.

Zhao, H. and Zheng, C. (2009b), "A new event-driven constant-volume method for solution of the time evolution of particle size distribution", *Journal of Computational Physics*, Vol. 228 No. 5, pp. 1412-1428.

Zhao, H., Zheng, C. and Xu, M. (2005a), "Multi-Monte Carlo approach for general dynamic equation considering simultaneous particle coagulation and breakage", *Powder Technology*, Vol. 154 No. 2, pp. 164-178.

Zhao, H., Zheng, C. and Xu, M. (2005b), "Multi-Monte Carlo method for coagulation and condensation/evaporation in dispersed systems", *Journal of Colloid and Interface Science*, Vol. 286 No. 1, pp. 195-208.

Zhou, K., Jiang, X. and Chan, T.L. (2020), "Error analysis in stochastic solutions of population balance equations", *Applied Mathematical Modelling*, Vol. 80, pp. 531-552.